Tjandra, N., Omichinski, J. G., Gronenborn, A. M., Clore, G. M., and Bax, A., 1997b, *Nature Struct. Biol.* **4:**732.
Venters, R. A., Metzler, W. J., Spicer, L. D., Mueller, L., and Farmer, B. T., II, 1995, *J. Am. Chem. Soc.* **117:**9592.
Vuister, G. W., Kim, S.-J., Wu, C., and Bax, A., 1994, *J. Am. Chem. Soc.* **116:**9206.
Wagner, G., Braun, W., Havel, T. F., Schaumann, T., Go, N., and Wüthrich, K., 1987, *J. Mol. Biol.* **196:**611.
Werner, M. H., Huth, J. R., Gronenborn, A. M., and Clore, G. M., 1995, *Cell* **81:**705.
Wittekind, M., Mapelli, C., Garmer, B. T., Suen, K.-L., Goldfarb, V., Tsao, J., Lavoie, T., Barbacid, M., Meyers, C. A., and Mueller, L., 1994, *Biochemistry* **33:**13531.
Wüthrich, K., 1986, *NMR of Proteins and Nucleic Acids*, Wiley, New York.
Xu, R. X., Word, J. M., David, D. G., Rink, M. J., Willard, D. H., and Gampe, R. T., 1995, *Biochemistry* **34:**2107.
Yu, H., Chen, J. K., Feng, S., Dalgarno, D. C., Brauer, A. W., and Schreiber, S. L., 1994, *Cell* **76:**933.
Zhang, H., Zhao, D., Revington, M., Lee, W., Jia, X., Arrowsmith, C., and Jardetzky, O., 1994, *J. Mol. Biol.* **238:**592.

2

Multidimensional ^{2}H-Based NMR Methods for Resonance Assignment, Structure Determination, and the Study of Protein Dynamics

Kevin H. Gardner and Lewis E. Kay

1. INTRODUCTION

1.1. Background: Deuteration prior to 1993

Over the past 30 years, deuterium labeling methods have played a critical role in solution NMR studies of macromolecules, in many cases improving the quality of spectra by both a reduction in the number of peaks and a concomitant narrowing of linewidths. Deuteration was initially used in a set of elegant experiments by the groups of Crespi and Jardetzky to reduce the complexity of one-dimensional (1D) ^{1}H spectra of proteins (Crespi and Katz, 1969; Crespi *et al.*, 1968; Markley *et al.*, 1968). To this end, highly deuterated proteins were produced by growing algae or

Kevin H. Gardner and Lewis E. Kay • Protein Engineering Network Centres of Excellence and Departments of Medical Genetics and Microbiology, Biochemistry, and Chemistry, University of Toronto, Toronto, Ontario M5S 1A8, Canada.

Biological Magnetic Resonance, Volume 16: Modern Techniques in Protein NMR, edited by Krishna and Berliner. Kluwer Academic / Plenum Publishers, 1999.

bacteria in D_2O media supplemented with either uniformly or selectively protonated amino acids. By monitoring the chemical shifts of the few remaining protons, conformational changes that occurred on ligand binding (Markley *et al.*, 1968) or oligomerization (Crespi and Katz, 1969) were investigated. Since these initial experiments, the preparation of proteins with amino acid selective protonation in a deuterated environment (or conversely, selective deuteration in an otherwise protonated molecule) has been regularly used for spectral simplification and residue type assignment (Oda *et al.*, 1992; Anglister, 1990; Arrowsmith *et al.*, 1990a; Brodin *et al.*, 1989).

In the 1980s, random fractional deuteration was employed to improve the quality of homonuclear proton two-dimensional (2D) NMR spectra. Because of the significantly lower gyromagnetic ratio of ^2H compared with ^1H ($\gamma[^2H]/\gamma[^1H]=0.15$), replacement of protons with deuterons removes contributions to proton linewidths from proton–proton dipolar relaxation and ^1H–^1H scalar couplings. At deuteration levels between 50–75%, the expected decrease in sensitivity related to the limited number of protons is offset to a large extent by a reduction in peak linewidths. Sensitivity gains were initially demonstrated in 1D ^1H spectra of the 43-kDa *E. coli* EF-Tu protein (Kalbitzer *et al.*, 1985) and subsequently in 2D homonuclear spectra of *E. coli* thioredoxin used for chemical shift assignment (LeMaster and Richards, 1988). Significant improvements have also been noted in many heteronuclear experiments. This is demonstrated for the case of an ^{15}N–^1H HSQC experiment in Fig. 1 where spectra recorded on fully protonated and perdeuterated samples (all nonexchangeable hydrogens substituted with deuterons) of a 30-kDa N-terminal domain of enzyme I of the *E. coli* phosphoenolpyruvate:sugar phosphotransferase system (EIN) are illustrated (Garrett *et al.*, 1997). As observed for the 14-kDa villin 14T protein (Markus *et al.*, 1994), deuterating all nonexchangeable sites to levels of 80–90% decreases amide proton transverse relaxation rates by approximately twofold. The improvement in sensitivity and resolution in the NH-detected dimension is particularly important because many classes of experiments record the amide proton chemical shift during acquisition (Clore and Gronenborn, 1994).

Deuteration can also improve the quality of NOESY experiments. In particular, substitution of aliphatic/aromatic protons with deuterons results in impressive sensitivity gains in NOESY spectra which record NH–NH correlations (LeMaster and Richards, 1988; Torchia *et al.*, 1988a). Initially demonstrated in perdeuterated systems, similar benefits have also been observed for proteins and peptides that are protonated at specific positions in an otherwise highly deuterated background (Pachter *et al.*, 1992; Reisman *et al.*, 1991; Arrowsmith *et al.*, 1990b; Tsang *et al.*, 1990). The sensitivity gains in these NOESY data sets are largely the result of reduced NH linewidths, as described above. However, the decrease in spin diffusion pathways and concomitant increase in selective T_1 values of the diagonal resonances also result in improvements. Moreover, it is possible to employ longer mixing times and, because of reduced spin diffusion rates, relate cross-peak intensities to internuclear distances more accurately than is possible from data recorded on highly protonated samples. This is of particular significance for longer range distance restraints. Finally, it is important to note that even in highly deuterated molecules the effects of spin diffusion cannot be neglected. In the case of highly deuterated proteins containing protonated amino acids, NOE spectra have been recorded with long mixing times to specifically promote intraresidue spin diffusion. In this way sidechain protons for several dimeric proteins with molecular masses above 20 kDa have been assigned (Reisman *et al.*, 1993; Arrowsmith *et al.*, 1990a,b).

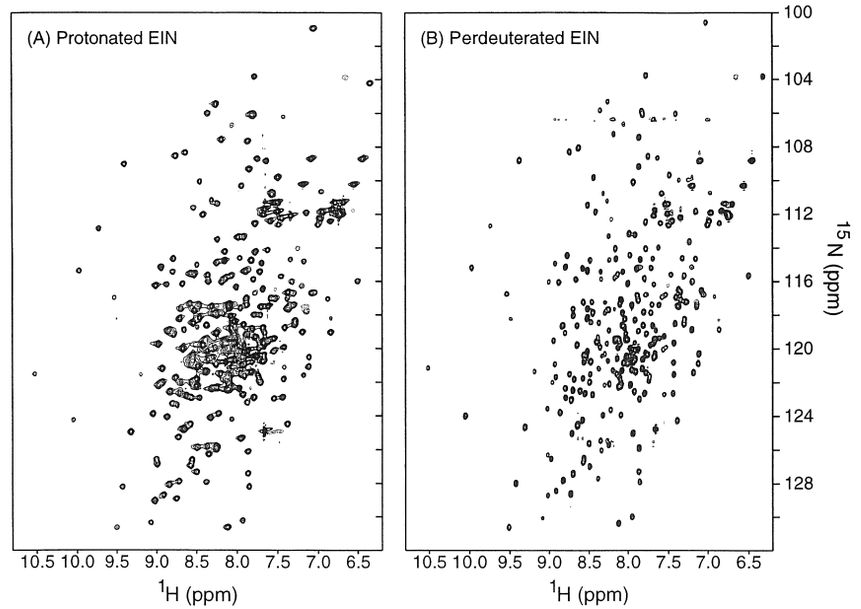

Figure 1. Effect of perdeuteration on the 2D ^{15}N–NH HSQC spectrum of the 30-kDa N-terminal domain of Enzyme I from the *E. coli* phosphoenolpyruvate-sugar phosphotransferase system. Both proteins are uniformly ^{15}N labeled, while the deuterated protein is approximately 90% uniformly deuterated. Reprinted with permission from Garrett *et al.* (1997).

1.2. Scope of This Review: Deuteration since 1993

As already described, deuteration can result in substantial improvements in NMR spectra used to study the structures of proteins and protein complexes. An alternative powerful strategy is triple resonance, multidimensional NMR spectroscopy of uniformly ^{15}N, ^{13}C labeled proteins (Bax, 1994; Clore and Gronenborn, 1994). In this approach sets of intra- and interresidue chemical shifts are correlated by transferring magnetization from one nucleus to another through one- or two-

bond scalar couplings. Data analysis from several of these experiments in combination facilitates the assignment of nitrogen, carbon, and proton chemical shifts of proteins with molecular masses of approximately 25 kDa or less. For systems larger than this, long molecular correlation times result in very efficient relaxation of the participating spins, especially ^{13}C nuclei, attenuating signal intensity and degrading spectral resolution.

A straightforward approach to decrease the relaxation rates of many of the nuclei that are key players in triple-resonance experiments is to substitute carbon-bearing protons with deuterons. At the field strengths currently in use, the major contribution to relaxation of carbon magnetization, for example, derives from one-bond $^{13}C-^{1}H$ dipolar interactions (Browne *et al.*, 1973; Allerhand *et al.*, 1971). In the case of a $^{13}C-^{1}H$ spin pair attached to a macromolecule, replacement of the proton with a deuteron attenuates the dipolar interaction by a factor of approximately 15. This results in a substantial lengthening of carbon relaxation times leading to improvements in the sensitivity of experiments relying on scalar-coupling-based transfers of magnetization involving carbon nuclei (Venters *et al.*, 1996; Yamazaki *et al.*, 1994a,b; Grzesiek *et al.*, 1993b; Kushlan and LeMaster, 1993b). The first demonstration of the utility of deuteration in concert with triple-resonance spectroscopy occurred in 1993 when Bax and co-workers described the 4D HN(COCA)NH experiment for correlating sequential amides. Subsequently a suite of triple-resonance experiments for assignment of backbone chemical shifts of deuterated proteins was developed and demonstrated on a 37-kDa protein/DNA complex (Yamazaki *et al.*, 1994a,b) and later extended for use on a 64-kDa version of this system (Shan *et al.*, 1996). The dramatic improvement in both the sensitivity and the resolution of triple-resonance spectra that deuteration provides is illustrated in Fig. 2 by comparing 2D $^{13}C/^{1}H$ projections of 3D HNCA spectra recorded on a fully protonated ^{15}N, ^{13}C labeled 23-kDa Shc PTB domain/peptide complex (a) and a 75% deuterated version of the same complex (b). The decrease in ^{13}C linewidth allows individual peaks to be resolved in the crowded center of these spectra and the improved signal-to-noise facilitates the observation of weaker cross-peaks.

A large number of triple-resonance pulse sequences have since been optimized for use on deuterated proteins (Section 3.2). The application of many of these methods to high-molecular-mass proteins (40 kDa and beyond) will require significant levels of deuteration. For example, complete assignment of ^{15}N, $^{13}C^{\alpha}$, $^{13}C^{\beta}$ and NH chemical shifts was achieved for a 37-kDa trp repressor/DNA ternary complex (Yamazaki *et al.*, 1994a,b) where the protein component was labeled at approximately 70%. However, a 90% deuteration level was required for similar studies on a 64-kDa trp repressor/DNA complex (Shan *et al.*, 1996). Regrettably, the advantages associated with deuteration are not without compromise. The substitution of deuterons for protons depletes the number of protons available for NOE-based interproton distance restraints. In the limiting case of perdeuteration, only exchangeable protons remain, resulting in a drastic reduction in both numbers and

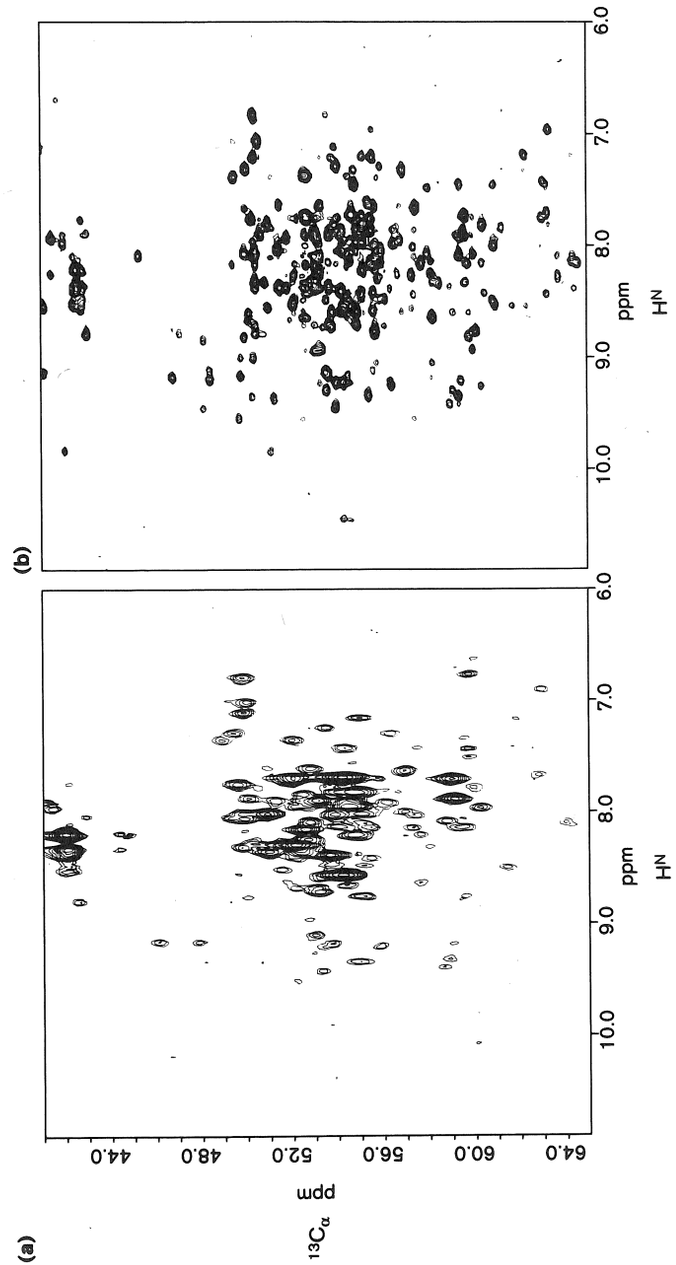

Figure 2. Comparison of 2D ($^{13}C_{\alpha}$, NH) projections from 3D HNCA spectra recorded of a 23-kDa Shc PTB domain/phosphotyrosine peptide complex. (a) ^{15}N, ^{13}C, ^{1}H uniformly labeled Shc PTB domain. (b) ^{15}N, ^{13}C, 75% ^{2}H uniformly labeled Shc PTB domain. Reprinted with permission from Sattler and Fesik (1996).

types of NOEs that can be measured in relation to fully protonated samples. It is not surprising, therefore, that structures determined from NOEs between backbone NH protons only have very low precision and accuracy (Gardner *et al.*, 1997; Smith *et al.*, 1996; Venters *et al.*, 1995b). This has stimulated the development of several different methods for the production of proteins that are selectively protonated at key positions in the molecule, allowing additional distance restraints to be measured, while maintaining a high level of deuteration at other sites so that experiments for sidechain and backbone assignment can enjoy the sensitivity gains that accompany deuteration.

To this point we have introduced the use of deuterium as an approach to improve the efficacy of large classes of triple-resonance experiments that would otherwise suffer significantly from relaxation loses. Outside of the low gyromagnetic ratio of the deuteron, no other properties of ^{2}H are exploited in these experiments. In contrast to the relatively recent use of deuterium in this role, the utility of ^{2}H NMR spectroscopy for the study of molecular dynamics has been recognized for several decades. Most of the work focused primarily on liquid-crystal samples, samples in the solid state, or solution state samples with deuterium labeling restricted to a small number of sites (Vold and Vold, 1991; Johnson *et al.*, 1989; Keniry, 1989; Keniry *et al.*, 1983; Schramm and Oldfield, 1983; Jelinski *et al.*, 1980; Seelig, 1977). Methods have emerged more recently for the measurement of sidechain dynamics properties of uniformly ^{13}C labeled, fractionally deuterated proteins through the indirect measurement of deuterium relaxation times, T_1 and $T_{1\rho}$ (Pervushin *et al.*, 1997; Kay *et al.*, 1996; Muhandiram *et al.*, 1995).

In this review, recent developments in the use of deuterium for studying protein structure and dynamics will be described. This includes the preparation of highly deuterated proteins, optimization of triple-resonance NMR experiments for use on highly deuterated samples, prospects for the structure determination of highly deuterated proteins, and the use of ^{2}H relaxation for the study of protein dynamics. The interested reader should consult previous reviews (LeMaster, 1994, 1990, 1989; Anglister, 1990) for a more thorough coverage of work in these fields prior to 1993.

2. DEUTERIUM LABELING METHODS

Proteins employed in NMR studies can be labeled using a number of different protocols that produce molecules with different patterns of deuterium incorporation. One labeling strategy results in deuterium incorporation throughout a protein in a roughly site-independent manner (uniform or random labeling) whereas a second approach produces a high level of deuteration (or protonation) at a restricted number of sites (site-specific labeling). The optimal labeling pattern for a particular sample is of course determined by the intended application(s). In what follows a number of methods are described for the generation of proteins deuterated on

aliphatic/aromatic carbon sites. Although considerable progress has been realized in the past several years in the production of uniformly deuterated (Batey *et al.*, 1996) or site-specifically deuterated (Földesi *et al.*, 1996; Ono *et al.*, 1996; Tolbert and Williamson, 1996; Agback *et al.*, 1994) nucleotides for use in NMR studies of RNA and DNA molecules, the present discussion will focus on protein applications exclusively.

2.1. Uniform Deuteration

As already mentioned, the optimal level of deuteration for a specific application, ranging from the complete substitution of protons with deuterons to moderate levels of fractional replacement, will very much depend on the experiments that are planned. Completely deuterated proteins have been used to eliminate contributions to spectra from one component of a macromolecular complex, as demonstrated in studies of a complex of fully deuterated calmodulin with a protonated peptide (Seeholzer *et al.*, 1986) and deuterated cyclophilin with protonated cyclosporin (Hsu and Armitage, 1992). However, a wider range of applications have made use of samples of (random) fractionally deuterated molecules. For example, random fractionally deuterated proteins were initially used to improve the sensitivity of 2D ^{1}H–^{1}H homonuclear spectra by reducing dipolar relaxation pathways, spin diffusion, and passive scalar couplings (LeMaster and Richards, 1988; Torchia *et al.*, 1988a). Fractional deuteration also significantly improves the sensitivity of many triple-resonance (^{15}N, ^{13}C, ^{1}H) experiments (Farmer and Venters, 1996; Nietlispach *et al.*, 1996; Shan *et al.*, 1996; Farmer and Venters, 1995; Yamazaki *et al.*, 1994a,b; Grzesiek *et al.*, 1993b), as will be discussed in greater detail in Section 3. In addition, the sidechain dynamics of proteins prepared in this manner can be studied using a number of new ^{13}C and ^{2}H spin relaxation experiments (Pervushin *et al.*, 1997; LeMaster and Kushlan, 1996; Muhandiram *et al.*, 1995; Kushlan and LeMaster, 1993a) as addressed in Section 5.

To a first approximation, randomly deuterated proteins can be generated in a straightforward manner. A culture of bacteria containing an overexpression vector for the protein of interest is grown in minimal media with the D_2O/H_2O ratio chosen to reflect the desired level of deuterium incorporation. Proteins generated will be composed of amino acids containing approximately the same deuterium content as in the overexpression media (see below). Cultures of simple eukaryotes such as algae and yeast can also grow in media containing up to 100% D_2O, facilitating the use of these organisms for the biosynthetic production of highly deuterated proteins (Crespi *et al.*, 1968; Katz and Crespi, 1966).

Expression of deuterated proteins in higher eukaryotic cells (plant and animal) is more challenging because these cells will not grow in media containing more than 30–50% D_2O (Katz and Crespi, 1966). This problem can be partially circumvented by culturing these cells in H_2O media supplemented with commercially

available ^{2}H-labeled algal amino acid extracts, analogous to previously established methods for expressing uniformly ^{15}N, ^{13}C, ^{1}H labeled proteins in these systems (Hansen *et al.*, 1992). Proteins produced in this manner will be highly deuterated at most carbon positions, although significant levels of potentially nondesired protonation can still occur through ^{2}H/^{1}H exchange with solvent protons, most notably at Cα sites.

Note that several factors can lead to a nonuniform distribution of deuterium throughout "randomly" fractionated proteins. In this regard, the carbon compounds used as growth substrates for *E. coli* are particularly important as protons from these molecules can be efficiently retained at specific sites within several amino acids. For example, proteins produced in bacteria grown in deuterated media containing ^{1}H-glucose typically have relatively high levels of protonation in sidechains of the aromatic amino acids. This results from the fact that aromatic groups are synthesized from glucose-derived carbohydrates (LeMaster, 1994). In certain cases, specific retention of protons from a protonated carbon source can be exploited to generate useful patterns of site-specific protonation within a highly deuterated background (Section 2.2.2). For applications requiring perdeuterated proteins, bacteria can be grown on deuterated carbon sources [e.g., ^{2}H-glucose or ^{2}H-succinate (LeMaster and Richards, 1988)] or simple protonated carbon sources where the carbon-bound protons are replaced by solvent deuterons prior to or during amino acid biosynthesis [e.g., ^{1}H-sodium acetate (Venters *et al.*, 1995a)].

Nonuniform deuteration can still be significant even when deuterated carbon sources exclusively are employed. Kinetic and thermodynamic isotope effects can alter the activity of metabolic and biosynthetic enzymes to the point of significantly biasing the distribution of deuterium in partially deuterated samples (Martin and Martin, 1990; Galimov, 1985). For example, a protein overexpressed in *E. coli* grown in an 80:20% D_2O:H_2O medium supplemented with deuterated succinate and 75% ^{2}H, DL-alanine was deuterated on average to a level of approximately 75% (LeMaster, 1997). However, specific sites within the protein had significantly lower ^{2}H incorporation, including the Ile γ1 methylene positions (< 50% deuterated). In another case, nonuniform type-specific deuterium incorporation has been observed in the CH_3:CH_2D:CHD_2 isotopomer distribution of methyl groups of an SH2 domain overexpressed in *E. coli* grown in 65:35% D_2O:H_2O medium (Kay *et al.*, 1996).

2.2. Site-Specific Protonation in a Highly Deuterated Environment

2.2.1. Protonated Amino Acid Sidechains in a Deuterated Background

In contrast to the approaches described above for producing proteins with deuterium substituted at an approximately uniform level throughout most of the aliphatic sites, proteins can also be generated where only specific sites are protonated in an otherwise highly deuterated background. Proteins can be labeled in this manner by overexpression in bacterial cultures grown in minimal D_2O media supplemented with protonated small organic molecules such as amino acids, amino acid precursors, or carbon sources (LeMaster, 1994, 1990). Alternatively, bacteria can be cultivated in H_2O-based media supplemented with deuterated algal cell lysates that have been chemically or enzymatically treated to promote site-specific protonation.

Some of the earliest ^{2}H-based NMR studies of proteins made use of deuterated, site-protonated molecules isolated from organisms grown in minimal media with high levels of D_2O and supplemented with fully or partially protonated amino acids (Crespi and Katz, 1969; Crespi *et al.*, 1968; Markley *et al.*, 1968). The resulting simplified 1D ^{1}H NMR spectra of these proteins facilitated the observation of well-separated peaks reporting on sites dispersed throughout the primary sequence of the molecule. Initial studies focused on the incorporation of leucine (Crespi *et al.*, 1968). Subsequently, most of the 20 natural amino acids have been successfully incorporated in this manner, either alone or in combination with other residues (Metzler *et al.*, 1996b; Smith *et al.*, 1996; Oda *et al.*, 1992; Brodin *et al.*, 1989). In general, wild-type strains of bacteria and algae can be used for amino acid specific labeling so long as the growth medium is supplemented with relatively high concentrations (> 30 mg/liter) of protonated compounds. In cases where it is necessary to use smaller amounts of these potentially expensive labeled compounds or to limit nondesirable labeling of amino acids derived from the labeled compound, amino acid-specific auxotrophic strains have been employed (Oda *et al.*, 1992; LeMaster, 1990). Similar approaches have also been used in the context of specific ^{15}N and ^{13}C labeling (Waugh, 1996; McIntosh and Dahlquist, 1990).

As previoulsy mentioned, proteins produced by bacteria in highly deuterated media containing a number of fully protonated amino acids usually retain most of the sidechain protons on these residues. In a typical D_2O-based growth medium, deuterons will replace between 30 and 80% of the Hα protons of the protonated amino acids (Metzler *et al.*, 1996b; Smith *et al.*, 1996; Crespi *et al.*, 1968), while the sidechains remain almost entirely protonated. On one hand, this high level of residual protonation is beneficial for the sensitivity of many proton-detected experiments. However, the presence of these spins can lead to rapid transverse relaxation rates for sidechain ^{13}C nuclei (Metzler *et al.*, 1996b; Smith *et al.*, 1996), reducing the sensitivity of triple-resonance experiments designed to assign sidechain chemical shifts, such as the HCC(CO)NH-TOCSY (Section 3.3). As well, protons located on the sidechain provide effective intraresidue spin diffusion pathways in NOE-based experiments, complicating the quantitation of cross-peak intensities in terms of internuclear distances (Pachter *et al.*, 1992).

2.2.2. Protonated Methyl Groups in a Deuterated Background: Pyruvate

To circumvent the problems associated with the use of fully protonated amino acids in the production of deuterated site-protonated proteins, Rosen and co-workers have developed a method that produces molecules with a more limited number of highly protonated sites (Rosen *et al.*, 1996). The approach involves growing bacteria in a D_2O-based minimal medium with a protonated nonglucose carbon source. As discussed in Section 2.1 for the case of glucose, the use of a protonated carbon source introduces protons at specific positions in various amino acids in a manner dependent on the details of the metabolism of the compound. Rosen *et al.* have taken advantage of the fact that the methyl group of pyruvate is the metabolic precursor of the methyls of Ala, Val, Leu, and Ile ($\gamma 2$ only) to produce proteins that are highly deuterated at all positions with the exceptions of the methyl groups mentioned above. In this approach, proteins are overexpressed in *E. coli* grown in a D_2O-based minimal medium with protonated pyruvate as the sole carbon source. The utility of this approach is demonstrated in Fig. 3, which compares ^{13}C–^{1}H HSQC spectra of ^{15}N, ^{13}C, fully protonated (a) and ^{15}N, ^{13}C, methyl protonated, highly deuterated (b) samples of the C-terminal SH2 domain of bovine phospholipase $C_{\gamma 1}$ (PLCC). The majority of the aliphatic sites in the pyruvate-derived protein are completely deuterated while the methyl groups of Ala, Val, Leu, and Ile ($\gamma 2$) are significantly protonated. However, the methylene groups of several amino acids identified in Fig. 3b are also protonated to a lower extent. It is noteworthy that the methyl peaks in the spectrum of the deuterated sample are highly asymmetric. This is the result of the production of CH_3, CH_2D, and CHD_2 isotopomers coupled with the significant one-bond deuterium isotope shift for both ^{13}C (–0.3 ppm per ^{2}H) and ^{1}H (–0.02 ppm per ^{2}H) (Gardner *et al.*, 1997). The extent of protonation for the pyruvate-derived methyl groups ranges from 40% (Ala) to 60% (Val and Ile) to 80% (Leu), as established on the basis of both mass spectrometry and NMR studies (Rosen *et al.*, 1996). These levels can be further increased by shortening the induction step during growth (Gardner *et al.*, 1996). The moderately high levels of protonation at Ala, Ile ($\gamma 2$), Val, and Leu methyl groups and the significant deuteration at most other sites (most notably, $C\alpha > 95\%$ and $C\beta > 80\%$ deuterated) ensure that high-sensitivity triple-resonance spectra both for backbone assignment and for correlation of sidechain ^{13}C and ^{1}H chemical shifts with backbone ^{15}N–^{1}H spin pairs can be obtained (Gardner *et al.*, 1996).

2.2.3. Protonated Methyl Groups in a Deuterated Background: Specifically Protonated Amino Acids and Amino Acid Precursors

Despite the utility of the pyruvate strategy described above, the presence of methyl isotopomers is limiting, in terms of both resolution and sensitivity. In addition, the level of protein produced in *E. coli* cultures grown in pyruvate-based

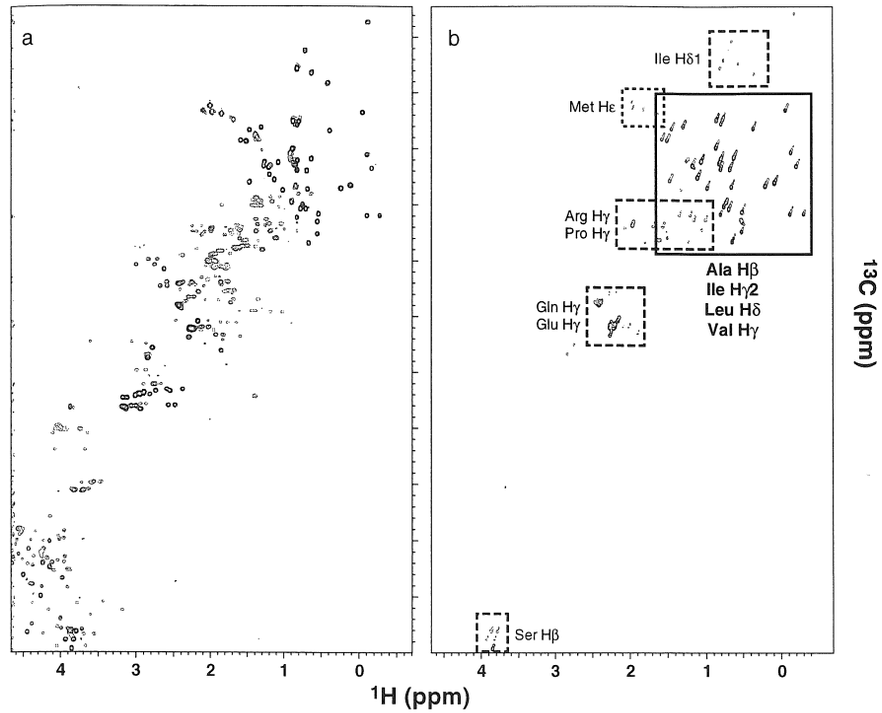

Figure 3. Constant time ^{13}C–^{1}H HSQC spectra of the PLCC SH2 domain prepared from (a) a fully protonated, H_2O medium with a ^{13}C-glucose carbon source and (b) a D_2O-based medium with ^{13}C, ^{1}H pyruvate the sole carbon source. Reprinted from Rosen *et al.* (1996).

media is approximately twofold reduced relative to cultures that use glucose as the carbon source. It is therefore necessary to develop an alternative approach in which proteins are overproduced in bacteria grown in a highly deuterated, glucose medium supplemented with amino acid precursors and amino acids that have useful patterns of protonation and deuteration. Both the precursors and the amino acids can be prepared *in vitro* using a combination of synthetic and enzymatic approaches with the conversion of the amino acid precursors to the appropriate amino acids occurring *in vivo* once the compounds are provided to *E. coli.* Intermediates can be chosen based on several criteria, including the ability to enter a biosynthetic pathway without complications from subsequent $^{1}H/^{2}H$ exchange reactions, the extent of *E. coli* assimilation and the ease of preparation. An example of this approach is illustrated in the production of proteins with high levels of deuteration at all positions with the exception of methyl positions of Val, Leu, and Ile ($\delta 1$ only) (Gardner and Kay, 1997). Proteins are overexpressed in *E. coli* grown in minimal

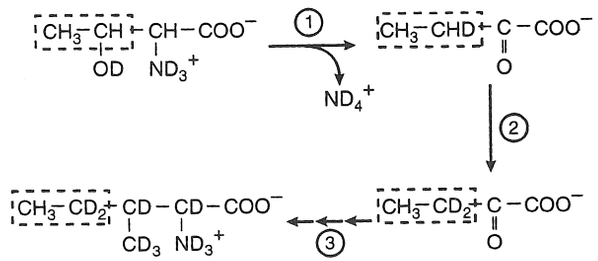

Figure 4. Generation of protein labeled with ^{13}C, ^{2}H (^{1}H-δ1 methyl) Ile. Step 1: *In vitro* conversion from Thr into [3-^{2}H] 2-ketobutyrate, catalyzed by *E. coli* biosynthetic threonine deaminase (Eisenstein, 1991). Step 2: *In vitro* conversion of [3-^{2}H] 2-ketobutyrate into [3,3-$^{2}H_2$] 2-ketobutyrate by proton/deuterium exchange at C3 using pH* 10.2, 45 °C. Step 3: *In vivo* conversion of [3,3-$^{2}H_2$] 2-ketobutyrate into Ile and eventual incorporation into overexpressed protein, carried out by *E. coli* metabolism. All steps performed in 99.5% D_2O. Reprinted with permission from Gardner and Kay (1997).

^{15}N, ^{13}C, ^{2}H medium containing deuterated glucose as the carbon source and supplemented with [2,3-$^{2}H_2$]-^{15}N, ^{13}C Val (available commercially) and [3,3-$^{2}H_2$]-^{13}C 2-ketobutyrate. Addition of [2,3-$^{2}H_2$]-Val to the growth medium (50 mg/liter, see below) results in the production of proteins in which both Val and Leu are highly deuterated at all nonmethyl positions, and in which only the CH_3 methyl isotopomer is produced. Ile, protonated only at the Cδ1 position, is generated using the set of reactions illustrated in Fig. 4. Commercially available ^{15}N, ^{13}C labeled Thr is the starting compound and is stoichiometrically converted to [3-^{2}H]-^{13}C 2-ketobutyrate in a process catalyzed by *E. coli* biosynthetic threonine deaminase. Note that because this reaction is carried out in D_2O, one of the two methylene hydrogens of 2-ketobutyrate becomes deuterated. Substitution of the remaining methylene proton with a deuteron is achieved via base-catalyzed exchange. The resultant product is sterile filtered and added without any further purification to a D_2O-based minimal medium supplemented with [2,3-$^{2}H_2$]-^{15}N, ^{13}C Val. A ^{13}C–^{1}H HSQC spectrum of the methyl region of the PLCC SH2 domain expressed from *E. coli* grown in this supplemented medium is shown in Fig. 5. Despite the fact that a prototrophic strain has been employed in the overexpression, over 90% of Val, Leu, and Ile in the protein is derived from the added Val and 2-ketobutyrate (Gardner and Kay, 1997). The nonmethyl Ile sidechain positions are highly deuterated and, as is the case with Val and Leu, only the CH_3 isotopomer is produced. In this particular example, fully protonated ^{15}N, ^{13}C Val has been used and therefore Val and Leu retain some protonation at the methine (Val β, Leu γ) positions. The undesired protonation can be eliminated by replacing the ^{15}N, ^{13}C Val added to the growth medium in the production of the SH2 domain with [2,3-$^{2}H_2$]-^{15}N,^{13}C Val, as discussed above. In this context, we have recently obtained a sample of the 40-kDa maltose-binding protein by overexpression in *E. coli* grown in minimal medium (D_2O) using ^{2}H, ^{13}C glucose and $^{15}NH_4Cl$ as the sole carbon and nitrogen sources and supplemented with [2,3-$^{2}H_2$]-^{15}N, ^{13}C Val and [3,3-$^{2}H_2$]-^{13}C 2-ketobutyrate. ^{13}C–^{1}H HSQC spectra have established the high level of protonation at methyl groups of Val, Leu, and Ile (δ1) and the very significant extent of deuteration at other carbon positions.

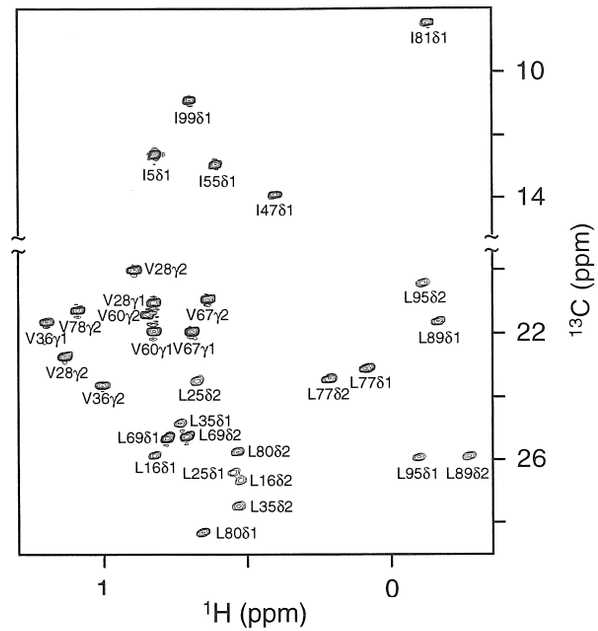

Figure 5. Methyl region of a ^{13}C–^{1}H constant-time HSQC spectrum of a highly deuterated, methyl-protonated PLCC SH2 domain, labeled using D_2O medium supplemented with ^{15}N, ^{13}C Val and [3,3-$^{2}H_2$]-^{13}C 2-ketobutyrate (Gardner and Kay, 1997). This protein is highly deuterated at all aliphatic sites except for the Val Cβ and Leu Cγ methine positions; these sites can be deuterated by the substitution of [2,3-$^{2}H_2$]-^{15}N, ^{13}C Val in place of ^{15}N,^{13}C Val. Over 90% of Val, Ile, and Leu derive from the added 2-ketobutyrate or Val. Reprinted with permission from Gardner and Kay (1997).

2.2.4. Protonated Cα in a Deuterated Background

While significant emphasis has been placed on producing highly deuterated proteins with protonation at select sidechain positions, methods have also emerged that place protons at specific backbone sites. Recently, Yamazaki *et al.* (1997) have produced a sample of the α subunit of *E. coli* RNA polymerase that is ^{15}N, ^{13}C, ^{2}H, $^{1}H\alpha$-labeled. By acetylating an ^{15}N, ^{13}C, ^{2}H-labeled amino acid mixture and hydrolyzing the resulting esters in H_2O under highly acidic conditions, the deuterons at the Cα positions of most amino acids are efficiently replaced by solvent

protons. The sidechain positions, however, remain highly deuterated during this procedure. The resulting mixture of ^2H, $^1H\alpha$ amino acids was added to *E. coli* growing in an H_2O-based minimal medium immediately prior to protein overexpression. Ten of the amino acid types in RNA polymerase produced in this manner were over 80% protonated at the Cα position and most sidechain positions retained high levels of deuteration. One drawback to this methodology in terms of cost effectiveness is that the ester hydrolysis step racemizes the Cα position; in principle this could be circumvented by the use of enzyme-based approaches (Homer *et al.*, 1993).

2.3. Practical Aspects of Producing Deuterated Proteins in *E. coli*

Although many of the labeling methods described above can be readily performed in any laboratory that routinely overexpresses proteins in bacterial systems, several aspects deserve special commentary. Figure 6 outlines the approach that we have used to generate both randomly deuterated and deuterated, site-protonated proteins.

At the outset of each growth, we use freshly transformed *E. coli* [typically but not exclusively strain BL21(DE3)] that has been plated onto solid H_2O-based rich medium. This is in contrast to approaches that utilize bacteria that have been previously adapted to growth in deuterated medium by culturing through steps with progressively higher percentages of D_2O (e.g., Venters *et al.*, 1995a) and then stored as glycerol stabs in a high-level D_2O medium. Because the culture is manipulated through multiple liquid medium steps (Fig. 6), we rely on several basic guidelines to ensure robust growth. All of the cultures are maintained at subsaturating cell densities, with optical densities measured at 600 nm (A_{600}) typically below 0.6. When the culture reaches this level the medium is briefly centrifuged and removed and the cells resuspended in an amount of fresh medium to bring the A_{600} to 0.05–0.1. In this manner, the culture is kept essentially in log-phase growth without significant lag periods. Note that the D_2O used during protein production can be recycled by flash chromatography to minimize the cost of this process (Moore, 1979).

It is extremely important that the composition of medium used in each step of the growth process be carefully regulated to ensure a constantly high growth rate. In particular, only one variable of the growth medium is changed (e.g., solvent or carbon source) between subsequent steps. As a result, we have found that we can completely change many variables (e.g., H_2O to D_2O or glucose to pyruvate) over the course of multiple steps without causing the bacterial culture to enter growth lag phases of longer than 1 to 2 h. Note that at least two D_2O growth steps occur prior to induction in each of the paths illustrated in Fig. 6, significantly minimizing the level of residual protonation in overexpressed proteins. With the typical dou-

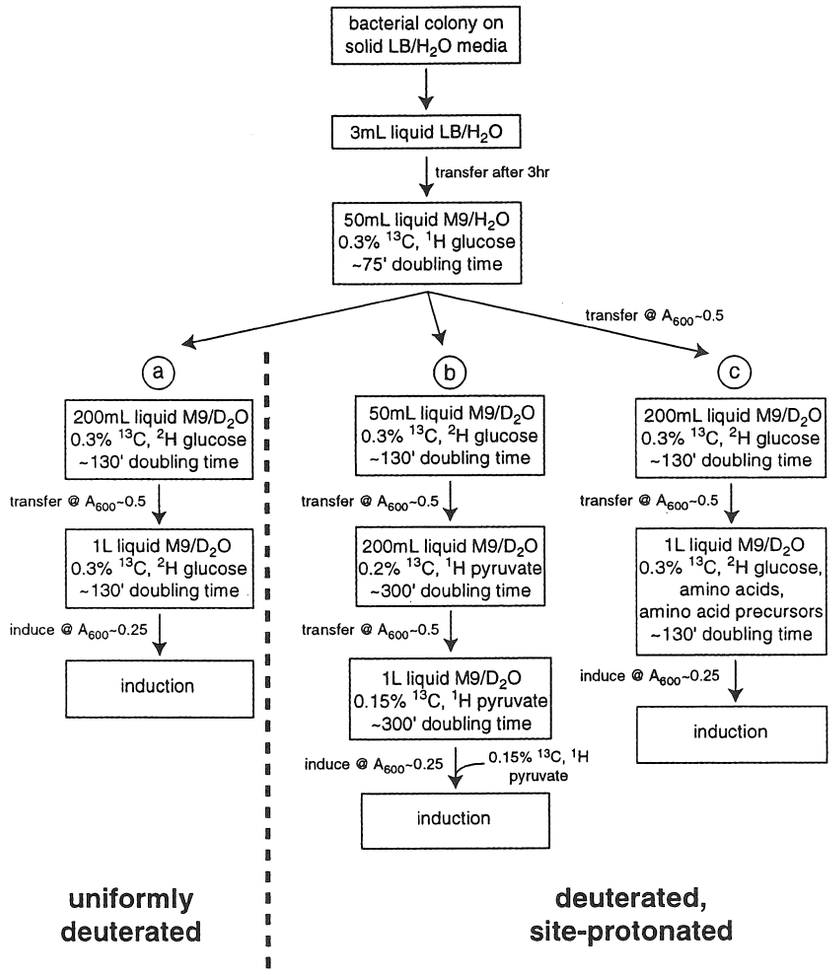

Figure 6. Typical bacterial growth protocols for producing highly deuterated proteins. (a) Uniformly deuterated protein production achieved by growing bacteria in D_2O medium (Section 2.1). (b) Production of deuterated, methyl-protonated protein at Ala, Val, Ile (γ2), and Leu sites using ^1H-pyruvate as a carbon source in a D_2O medium (Section 2.2.2). A total concentration of 0.3% ^1H-pyruvate is used in the final induction culture, added incrementally as described in Rosen *et al.* (1996). (c) Production of deuterated, methyl-protonated protein at Val, Ile (δ1), and Leu sites using protonated amino acids or amino acid precursors in a D_2O medium (Section 2.2.3). In all cases, ^2H-labeled glucose should be used for steps in D_2O medium to obtain as uniform a level of deuteration as possible. M9 is defined as the medium without the carbon source.

bling times indicated on the figure for bacterial cultures grown at 37 °C, a usual growth requires between 18 and 60 h.

The purification of a highly deuterated protein is essentially unchanged relative to procedures used for the corresponding protonated versions of the molecule. It is important to recognize that proteins synthesized in D_2O will typically retain deuterons at a significant fraction of backbone amide sites even though purification takes place in H_2O-based buffers. Introduction of protons at labile sites can be achieved by a denaturation/renaturation cycle of the protein in an H_2O-containing buffer using chemical denaturants such as guanidine hydrochloride or urea (Constantine *et al.*, 1997; Venters *et al.*, 1996). Alternatively, thermostabile proteins can be incubated at high temperatures for extended periods of time to catalyze NH exchange.

3. TRIPLE-RESONANCE METHODS

3.1. General Comments

Despite the demonstrated utility of triple-resonance (^{15}N, ^{13}C, ^{1}H) methods for structural studies of proteins, a number of significant limitations occur when these techniques are applied to proteins or protein complexes with molecular masses in excess of approximately 20 kDa. The first problem relates to the rapid relaxation rates of many of the nuclei that participate in the magnetization transfer steps that occur during the course of these complex pulse sequences. The situation is particularly acute in the case of ^{13}C spins, where, for example, $^{13}C\alpha$ transverse relaxation times are on the order of 16 ms for a protein tumbling with a correlation time of 15 ns (Yamazaki *et al.*, 1994a). The second limiting feature is the lack of resolution in spectra (in particular in carbon dimensions), to a large extent the product of short acquisition times that are necessitated by rapid transverse relaxation rates. As described in Section 1 and illustrated in Fig. 7 for the case of a $^{13}C\alpha$ carbon with a single attached hydrogen, deuteration of carbon sites provides a solution to these problems. Figure 7 compares carbon linewidths for a carbon–hydrogen spin pair as a function of molecular correlation time, where relaxation contributions to the ^{13}C spin from chemical shift anisotropy, $^{13}C\alpha$–$^{1}H\alpha$ or $^{13}C\alpha$–$^{2}H\alpha$ dipolar interactions are considered. It is clear in the case of a ^{13}C–^{1}H pair that the dominant interaction is dipolar and that this effect can be largely suppressed through deuteration. For example, for a molecular correlation time of 14.5 ns, deuteration is predicted to increase the carbon transverse relaxation time from 16.8 ms (^{13}C–^{1}H) to 257 ms (^{13}C–^{2}H), where only one-bond ^{13}C–^{1}H/^{13}C–^{2}H dipolar effects have been considered. When contributions from additional dipolar interactions involving the adjacent carbonyl, $^{13}C\beta$, and ^{15}N spins as well as chemical shift anisotropy are included, the predicted carbon transverse relaxation time decreases from 257 ms to

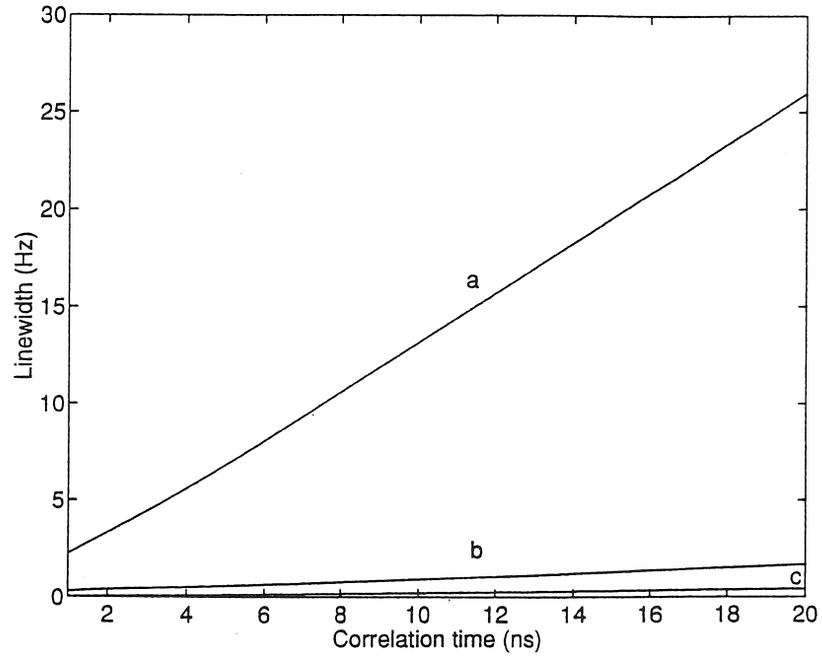

Figure 7. Expected contributions to the $^{13}C\alpha$ linewidth from dipolar and CSA relaxation mechanisms assuming an isolated $^{13}C\alpha$–$^{1}H\alpha$ or $^{13}C\alpha$–$^{2}H\alpha$ spin pair as part of an isotropically tumbling molecule in solution. (a) Contribution to the $^{13}C\alpha$ linewidth from $^{13}C\alpha$–$^{1}H\alpha$ dipolar interactions (assuming a carbon–proton separation of 1.10 Å). (b) Contribution from $^{13}C\alpha$–$^{2}H\alpha$ dipolar interactions. (c) Contribution from $^{13}C\alpha$ CSA (assuming an axially symmetric $^{13}C\alpha$ CSA tensor, $\Delta\sigma$ = 34 ppm). Reprinted with permission from Yamazaki *et al.* 1994a).

approximately 160 ms. Experimentally, transverse relaxation times were found to increase from 16.5 ± 3 ms to 130 ± 12 ms in the case of an ^{15}N, ^{13}C, ~70% ^{2}H labeled 37-kDa trpR/unlabeled DNA complex (correlation time of 14.5 ± 0.9 ns) (Yamazaki *et al.*, 1994a). The discrepancy between calculated and experimental values (160 ms versus 130 ms) is likely the result of the residual 30% protonation.

Substitution of deuterons for protons has a second major benefit as well. The significant decrease in carbon linewidths in deuterated proteins facilitates the use of constant-time carbon acquisition periods (Santoro and King, 1992; Vuister and Bax, 1992). For many experiments, such as the CT-HNCA and CT-HN(CO)CA, this period is set to $1/J_{CC}$, where J_{CC} is the one-bond ^{13}C–^{13}C homonuclear scalar coupling (Yamazaki *et al.*, 1994a,b). In addition to improving resolution by allowing significantly longer acquisition times than would otherwise be possible, the deleterious effects of passive one-bond carbon couplings on spectral resolution and sensitivity can be eliminated (Section 3.2).

A wide variety of triple-resonance pulse schemes have been modified to take advantage of reduced ^{13}C relaxation rates in highly deuterated proteins. Table 1 provides a listing of many of these experiments. In general, only minor changes are required to adapt a pulse sequence for use on deuterated proteins. Primarily these changes include the use of deuterium decoupling (Section 3.4) and, in some cases, the incorporation of various elements such as constant-time indirect detection periods, which likely would result in unacceptable sensitivity losses in experiments on protonated proteins. Specific modifications tailored to particular samples are also possible, such as pulse schemes developed for use on highly deuterated, site-protonated proteins including deuterated, methyl-protonated (Gardner *et al.*, 1996; Rosen *et al.*, 1996) and deuterated, Hα-protonated (Yamazaki *et al.*, 1997) molecules.

The fact that it is possible, at least in principle, to generate deuterated samples with high occupancy of protons at the labile sites in the molecule has resulted in the design of many experiments that are of the "out-and-back" variety where magnetization both originates and is detected on NH spins (Yamazaki *et al.*, 1994a,b). These experiments are performed on samples dissolved in H_2O and benefit by the relatively good dispersion of cross-peaks in ^{15}N, NH correlation spectra. Alternatively, a different strategy is required for samples in which the Hα site is protonated in proteins that are otherwise highly deuterated. In this case "out-and-back" experiments have been developed where the role of the NH spin discussed above is replaced by the Hα nucleus (Yamazaki *et al.*, 1997). Experiments of this type are best conducted in D_2O. It must be noted that a drawback of deuteration in all experiments is that the T_1 relaxation times of the remaining protons are significantly increased, requiring the use of longer recycle delays than typically employed in experiments performed with protonated molecules (Nietlispach *et al.*, 1996; Markus *et al.*, 1994; Yamazaki *et al.*, 1994a).

3.2. Backbone Chemical Shift Assignment

A large number of experiments for assignment of backbone chemical shifts have been developed for use on deuterated proteins, with many of these pulse schemes analogous to versions used for protonated samples. In addition to the 4D HN(COCA)NH described first by Bax and co-workers (Grzesiek *et al.*, 1993b) and the suite of experiments for correlating backbone $^{13}C\alpha$, ^{15}N, NH, and sidechain $^{13}C\beta$ chemical shifts designed by Yamazaki *et al.* (1994a,b), several other groups have published pulse schemes optimized for use on deuterated molecules. Experiments include the HN(CA)CO (Matsuo *et al.*, 1996a,b), HN(CA)NH (Ikegami *et al.*, 1997), alternative HN(COCA)NH sequences (Matsuo *et al.*, 1996a; Shirakawa *et al.*, 1995), as well as schemes providing backbone correlations with residue-selective editing (Dötsch *et al.*, 1996). To illustrate a number of the features that are particular to pulse schemes optimized for use on deuterated

Table 1
Triple-resonance NMR Methods with Versions Optimized for Use with Highly Deuterated Proteins

Method	References
Backbone	
Out-and-back	
3D CT-HNCA	Yamazaki *et al.* (1994b)
3D CT-HN(CO)CA	Yamazaki *et al.* (1994a)
3D HN(COCA)CB	Yamazaki *et al.* (1994a)
3D HN(CA)CB	Yamazaki *et al.* (1994a)
4D HNCACB	Yamazaki *et al.* (1994a)
3D CT-HN(COCA)CB	Shan *et al.* (1996)
3D CT-HN(CO)CA	Shan *et al.* (1996)
3D HN(CA)CO	Matsuo *et al.* (1996a,b)
3D HACAN	Yamazaki *et al.* (1997)
3D HACACO	Yamazaki *et al.* (1997)
3D HACACB	Yamazaki *et al.* (1997)
3D HACA(N)CO	Yamazaki *et al.* (1997)
Straight-through	
3D, 4D HN(COCA)NH	Grzesiek *et al.* (1993b), Shirakawa *et al.* (1995), Matsuo *et al.* (1996a)
4D HN(CA)NH	Ikegami *et al.* (1997)
4D HBCB/HACANNH	Nietlispach *et al.* (1996)
4D HBCB/HACA(CO)NNH	Nietlispach *et al.* (1996)
Sidechain	
Out-and-back	
2D H_2N-HSQC	Farmer and Venters (1996)
3D $H_2N(CO)C_{\gamma/\beta}$	Farmer and Venters (1996)
3D $H_2N(COC_{\gamma/\beta})C_{\beta/\alpha}$	Farmer and Venters (1996)
2D $H(N_{\varepsilon/\eta})C_{\delta/\varepsilon}$	Farmer and Venters (1996)
2D $H(N_{\varepsilon/\eta}C_{\delta/\varepsilon})C_{\gamma/\beta}$	Farmer and Venters (1996)
2D $H(N_{\varepsilon})C_{\zeta}$	Farmer and Venters (1996)
$H(N_{\varepsilon/\eta})C_{\zeta}$	Farmer and Venters (1996)
Straight-through	
3D C(CC)(CO)NH	Farmer and Venters (1995)
4D HCC(CO)NH	Nietlispach *et al.* (1996)
3D (H)C(CO)NH-TOCSY	Gardner *et al.* (1996)

samples, we provide a brief description of the CT-HNCA (Yamazaki *et al.*, 1994b). This experiment correlates the chemical shifts of intraresidue ^{15}N–NH spin pairs of residue i with the $^{13}C\alpha$ shifts of residues i and $(i-1)$. Figure 8 presents the pulse sequence of the CT-HNCA experiment (Yamazaki *et al.*, 1994b); it is clear that many of the magnetization transfer steps are identical to those employed in the

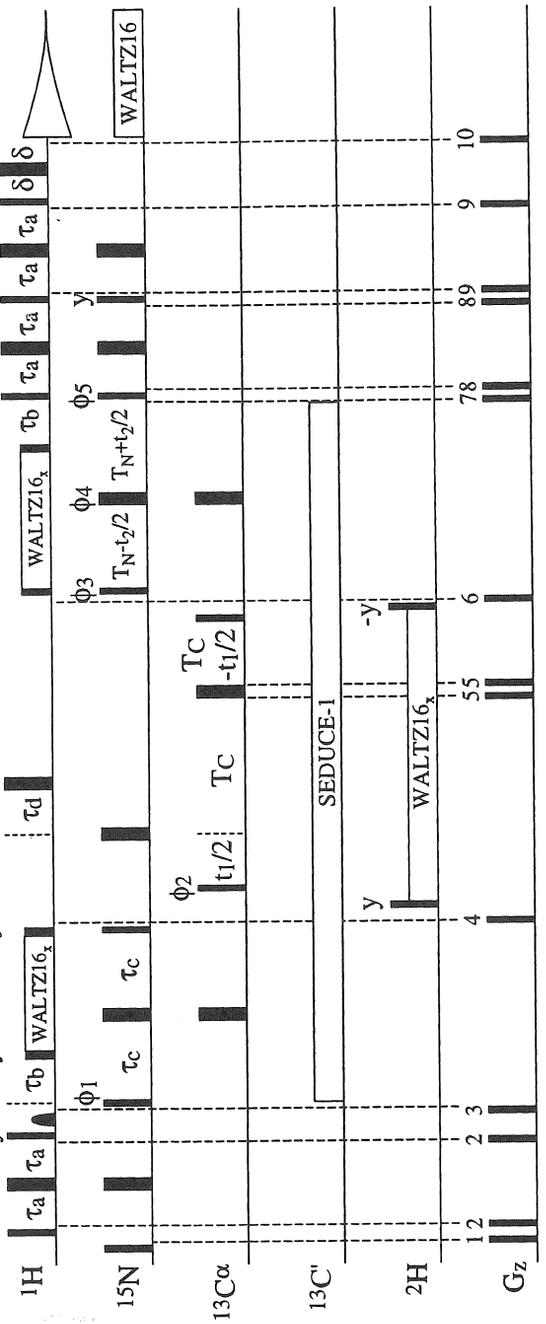

Figure 8. Pulse sequence for the CT-HNCA experiment for use on uniformly ^{15}N, ^{13}C, fractionally ^{2}H labeled proteins. Correlations linking ^{15}N,NH spin pairs with intra- (*i*) and inter-residue (*i* – 1) ^{13}Cα chemical shifts are provided by this experiment. Reprinted with permission from Yamazaki *et al.* (1994b) and modified by the addition of 90° pulses on both sides of the ^{2}H WALTZ-16 decoupling field.

HNCA experiment developed for ^{15}N, ^{13}C, ^{1}H samples (Grzesiek and Bax, 1992; Ikura *et al.*, 1990; Kay *et al.*, 1990). Schematically, these steps can be diagrammed as

$$NH(i) \xrightarrow{J_{NH}} {}^{15}\mathrm{N}(i) \xrightarrow{J_{NC}} {}^{13}\mathrm{C}\alpha(i, i-1)\ [t_1] \xrightarrow{J_{NC}} {}^{15}\mathrm{N}(i)\ [t_2] \xrightarrow{J_{NH}} \mathrm{NH}(i)\ [t_3]$$

where t_1, t_2, and t_3 are acquisition periods and the active couplings involved in each transfer step are indicated above the arrows. Fourier transformation of the resultant time domain data set gives a frequency domain map with both intra- (one bond) and inter- (two bond) correlations of the form (^{13}Cα, ^{15}N, NH). It is noteworthy that both ^{13}Cα and ^{15}N chemical shifts are recorded in a constant-time manner. During the carbon constant-time period, evolution of magnetization related to the passive one-bond ^{13}C–^{13}C scalar coupling proceeds according to the relation, $\cos^{N}(2\pi J_{CC}T_C)$, where $N = 0$ for Gly and 1 for all other amino acids. Because J_{CC} values connecting aliphatic carbons are essentially uniform, it is possible to refocus the effects of such couplings by choosing $2T_C$ to be a multiple of $1/J_{CC}$ (Santoro and King, 1992; Vuister and Bax, 1992). In practice, $2T_C$ is set to $1/J_{CC}$ (28 ms) so as to minimize signal attenuation caused by relaxation. In this regard, deuteration is critical, for in proteins of even modest size transverse relaxation of ^{13}Cα carbons can become limiting. For example, consider a protein with a correlation time of 14.5 ns, such as the 37-kDa trpR/DNA complex studied by Jardetzky and co-workers (Zhang *et al.*, 1994; Arrowsmith *et al.*, 1990a) and Yamazaki *et al.* (1994a,b). Assuming average ^{13}Cα T_2 values of 16 ms and 130 ms for protonated and deuterated samples, respectively, relaxation during the constant time period attenuates the final signal by factors of 5.8 and 1.2, respectively. In the case of the trpR/DNA complex described above, deuteration was critical for the complete assignment of backbone chemical shifts using triple-resonance methods.

A number of additional features relating to the sensitivity of the pulse scheme of Fig. 8 are worthy of comment. First, signal-to-noise can be improved by minimizing saturation and/or dephasing of the water signal (Kay *et al.*, 1994; Stonehouse *et al.*, 1994; Grzesiek and Bax, 1993). This is achieved by ensuring that water magnetization is placed along the +*z* axis prior to the application of homospoil gradients and immediately prior to signal detection. Maintaining a reservoir of water magnetization is critical, especially in experiments performed on highly deuterated proteins where magnetization originates on NH spins. In this case, exchange between water and labile sites can increase the rate at which NH magnetization is replenished (Stonehouse *et al.*, 1994), circumventing to some extent the limitations imposed by long T_1 values on repetition delays. Second, as described in some detail in Section 3.4, it is essential that deuterium decoupling be employed during periods in which transverse carbon magnetization is present. The deuterium decoupling element is sandwiched between ^{2}H 90° pulses that place ^{2}H

magnetization collinear with the decoupling field (Farmer and Venters, 1995; Muhandiram *et al.*, 1995). In this manner, the magnetization is restored to the $+z$ axis after decoupling, minimizing lock instability. Note the analogous use of ^{1}H 90° pulses flanking the WALTZ-16 decoupling elements in the CT-HNCA sequence, which minimizes scrambling of water caused by nonintegral multiples of the WALTZ scheme (Kay *et al.*, 1994). Third, an enhanced sensitivity pulsed field gradient approach is employed to select for ^{15}N magnetization during the nitrogen constant-time period. The use of gradients to select for coherence transfer pathways and a discussion of the classes of experiments and the molecular masses for which the enhanced sensitivity method is beneficial are deferred until Section 3.5.

As a final point of interest, it is noteworthy that an ^{1}H 180° pulse is applied at a time of $t_1/2 + \tau_d$ after the start of the carbon constant-time period. By choosing τ_d to be $1/(4J_{CH})$, where J_{CH} is the magnitude of the one-bond ^{13}C–^{1}H scalar coupling, carbon magnetization from ^{13}C–^{1}H spin pairs evolves for a net duration of $1/(2J_{CH})$ during this constant-time interval and is not refocused into observable signal by the application of the remaining pulses in the sequence. In the case where the experiment is performed on perdeuterated molecules, this pulse is not necessary. However, in applications to fractionally deuterated proteins it may be possible to observe signals from both ^{13}C–^{1}H and ^{13}C–^{2}H pairs, arising from residues with high levels of mobility and hence decreased carbon relaxation rates. The doubling of signals degrades resolution in the carbon dimension of the HNCA spectrum and application of this pulse is thus recommended in these cases.

As described above, many of the triple-resonance pulse schemes that are currently employed for the assignment of deuterated proteins record backbone and sidechain carbon chemical shifts and in these cases deuterium decoupling during carbon evolution is necessary. However, in special classes of experiments it is possible to eliminate deuterium decoupling through the use of magnetization transfer schemes that rely on carbon cross-polarization. For example, in a version of the HN(COCA)NH experiment proposed by Shirakawa *et al.* (1995), magnetization is transferred from ^{13}CO to ^{13}Cα spins and subsequently from ^{13}Cα to ^{15}N using cross-polarization sequences. This circumvents the need for deuterium decoupling, which would otherwise be necessary during the relay from carbon to nitrogen if INEPT-based magnetization transfer methods had been employed (Grzesiek *et al.*, 1993b).

Recently, Yamazaki's group has described a suite of pulse sequences for use with highly deuterated, Cα-protonated samples (Yamazaki *et al.*, 1997). The experiments are of particular value in cases where rapid exchange with water precludes the use of NH-based schemes. In a manner analogous to the CT-HNCA sequence described above, carbon chemical shift is recorded in a constant-time manner. To minimize the rapid decay of carbon magnetization during this period, double- and zero-quantum ^{13}C, ^{1}H coherences are established. It is straightforward to show that in the macromolecule limit the relaxation of these two-spin coherences

proceeds in a manner that is independent of the large ^{13}C–^{1}H one-bond dipolar interaction (Griffey and Redfield, 1987). In the case of a protonated sample the advantages of using double- and zero-quantum coherences are offset to some extent by relaxation of the participating proton with proximal proton spins. Additionally, homonuclear proton couplings that evolve during the constant-time carbon evolution period further attenuate the signal (Grzesiek and Bax, 1995). Because the molecules prepared by Yamazaki *et al.* are deuterated at all non-Cα positions, pulse schemes that make use of this approach enjoy benefits that are seldom realized in applications involving protonated samples. For example, increases in relaxation times of approximately a factor of 4.5 (double/zero versus carbon single quantum) have been realized for the carboxy-terminal domain of the α subunit of *E. coli* RNA polymerase at 10 °C (correlation time of 17 ns).

3.3. Sidechain Chemical Shift Assignment

Two of the most often used experiments for the assignment of aliphatic sidechain chemical shifts in protonated, ^{15}N, ^{13}C-labeled proteins are the (H)C(CO)NH- and H(CCO)NH-TOCSY (Grzesiek *et al.*, 1993a, Logan *et al.*, 1993, 1992; Montelione *et al.*, 1992). In these pulse schemes, magnetization originating on sidechain protons is relayed via a carbon TOCSY step to the backbone Cα position and finally transferred to the ^{15}N, NH spins of the subsequent residue. The experiments provide correlations linking either aliphatic protons or carbons with backbone amide shifts or in the case of a 4D sequence developed by Fesik and co-workers (Logan *et al.*, 1992) connectivities are established between all four groups of spins (^{13}C, ^{1}H, ^{15}N, NH). The large number of transfer steps involved in the relay of magnetization from sidechain to backbone sites in these experiments limits their utility to proteins or protein complexes with molecular masses on the order of 20 kDa or less. Nietlispach *et al.* (1996) have developed a number of experiments for sidechain assignment in fractionally deuterated proteins and suggest that deuteration levels on the order of 50% provide a good balance between the need for aliphatic protons and the requirement of decreased carbon relaxation rates.

Farmer and Venters have developed a number of experiments for sidechain assignment in highly deuterated proteins. In one such scheme, a simple modification to the original (H)C(CO)NH-TOCSY is made allowing magnetization to originate on (deuterated) aliphatic carbon sites (Farmer and Venters, 1995). The utility of this sequence has been demonstrated in spectacular fashion on a perdeuterated sample of human carbonic anhydrase (HCA II, 29 kDa) allowing essentially complete assignment of sidechain carbon chemical shifts. A number of experiments for assignment of sidechain ^{15}N/NH resonances in highly deuterated samples have also been published by this group (Farmer and Venters, 1996). These triple-resonance sequences rely on correlating sidechain ^{15}N–NH pairs

with carbon shifts that have been previously assigned using the experiment(s) discussed above. Because deuteration limits the number of available NOEs for structure determination, it is important that as many of the remaining protons in the molecule as possible be assigned. In this context, the assignment of Arg, Gln, and Asn labile sidechain protons is crucial.

3.4. Deuterium Decoupling

In the extreme narrowing limit, the ^{13}C spectrum of an isolated ^{13}C–^{2}H spin pair consists of a triplet, with each multiplet component separated from its nearest neighbor by J_{CD}, where J_{CD} is the magnitude of the one-bond ^{13}C–^{2}H scalar coupling. As the tumbling time of the molecule to which the ^{13}C–^{2}H pair is attached increases, the ^{2}H T_1 relaxation time decreases and the multiplet structure collapses in the vicinity of the T_1 minimum. In the slow correlation time limit, linewidths of the components narrow and the multiplet component structure becomes decidedly asymmetric as a result of cross-correlation between ^{13}C–^{2}H dipolar and ^{2}H quadrupolar relaxation interactions (Murali and Rao, 1996; Grzesiek and Bax, 1994; London *et al.*, 1994; Kushlan and LeMaster, 1993b). Finally, at very long correlation times the outer components disappear completely.

The deleterious effects of deuterium spin flips on ^{13}C spectra of deuterated proteins were recognized over two decades ago by Browne *et al.* (1973), who suggested the use of high-power deuterium decoupling as a means of reducing carbon linewidths. However, at that time the power levels required for efficient decoupling could not be achieved. The increase in ^{2}H T_1 relaxation times at the magnetic field strengths typically in use today coupled with the higher decoupling power levels that are available on commercial spectrometers have led to the successful use of deuterium decoupling in triple resonance NMR applications, first demonstrated by Bax and co-workers in 1993 (Grzesiek *et al.*, 1993b).

3.5. The Use of Enhanced Sensitivity Pulsed Field Gradient Coherence Transfer Methods for Experiments on Large Deuterated Proteins

It has long been recognized that pulsed field gradients could be used both to select for desired coherence transfer pathways and reject others (Bax *et al.*, 1980; Maudsley *et al.*, 1978) and to reduce the artifact contact in spectra (Keeler *et al.*, 1994). However, the use of this technology in high-resolution NMR spectroscopy had to await the development of probes with actively shielded gradient coils in the early 1990s; since then, the use of gradients has become widespread. Many of the initial applications to macromolecules employed gradients to select for coherence transfer pathways (Boyd *et al.*, 1992; Davis *et al.*, 1992; Tolman *et al.*, 1992), following on the pioneering work of Ernst and co-workers (Maudsley *et al.*, 1978) and Bax *et al.* (1980). A significant limitation associated with these early experiments is that only one of the two paths that normally contribute to the observed signal in non-gradient-based experiments was observed, reducing sensitivity (Kay, 1995a,b). More recently, building on the enhanced sensitivity nongradient methods of Rance and co-workers (Palmer *et al.*, 1991b; Cavanagh and Rance, 1988), gradient-based pulse schemes with pathway selection that do not suffer from the abovementioned sensitivity losses have been developed (Muhandiram and Kay, 1994; Schleucher *et al.*, 1994, 1993; Kay *et al.*, 1992b). In the absence of relaxation and pulse imperfections, the proposed methods are a full factor of 2 more sensitive than their counterparts that employ gradients for coherence transfer selection but do not make use of enhanced sensitivity and a factor of $\sqrt{2}$ more sensitive than nongradient experiments.

The sensitivity advantages associated with enhanced sensitivity pulsed field gradient coherence transfer selection in triple-resonance-based NH-detected spectroscopy have been described for applications to fully protonated, ^{15}N, ^{13}C labeled molecules ranging in size from approximately 10 to 20 kDa (Muhandiram and Kay, 1994). On average, gains of approximately 15–25% were noted in relation to nongradient methods. The decrease in sensitivity relative to the expected theoretical enhancement of $\sqrt{2}$ is largely the result of relaxation losses that occur during the increased number of delays in these experiments. As these losses are most severe for large molecules, it is important to establish the molecular mass limit above which the sensitivity advantages of this method are marginal. In this regard Shan *et al.* have compared signal-to-noise ratios of HNCO spectra recorded both with and without enhanced sensitivity methods (Shan *et al.*, 1996). An ^{15}N, ^{13}C, ~80% ^{2}H sample of the PLCC SH2 domain was prepared in either 0, 15, or 30% glycerol; the steep viscosity dependence of glycerol with temperature permits convenient manipulation of the overall correlation time of the SH2 domain, allowing spectra to be recorded as a function of "effective molecular mass." Statistically significant sensitivity gains were observed for correlation times as large as 21 ns. It is noteworthy that the enhancements in triple-resonance-based spectra are likely to be larger than in ^{15}N–NH HSQC spectra, as the ^{15}N chemical shift is not recorded in a constant-time manner in the latter experiment. Thus, additional delays must be included during ^{15}N evolution to allow for the application of coherence transfer selection gradients without the introduction of phase distortions resulting from chemical shift evolution. Finally, signal-to-noise advantages mentioned above in the context of highly deuterated proteins will be larger than for protonated molecules. As discussed in Section 1.1, deuteration increases transverse relaxation times of NH protons by approximately a factor of 2 (Venters *et al.*, 1996; Markus *et al.*, 1994). This has a particularly significant effect on the efficiency of sensitivity enhancement-based experiments, which, relative to other classes of experiments, rely on increased delay times during which NH magnetization evolves. It must be emphasized that even in the absence of notable sensitivity gains there are advantages

in gradient-based coherence transfer selection methods, including artifact and solvent suppression and minimization of phase cycling.

3.6. Deuterium Isotope Effects on ^{13}C and ^{15}N Chemical Shifts

Along with the benefits that deuterium substitution provides in terms of the reduction of heteronuclear transverse relaxation rates comes the not so desired perturbation of the chemical shifts of ^{15}N and ^{13}C nuclei. These so-called deuterium isotope shifts are significant for ^{15}N and ^{13}C spins located within at least three bonds of the site of deuteration (Hansen, 1988). In an effort to quantitate the magnitude of one- [$^1\Delta\ ^{13}C(^2H)$], two- [$^2\Delta\ ^{13}C(^2H)$], and three-bond [$^3\Delta\ ^{13}C(^2H)$] deuterium isotope effects on ^{13}C chemical shifts, Venters *et al.* (1996) and Gardner *et al.* (1997) have compared chemical shifts of $^{13}C\alpha$ and $^{13}C\beta$ carbons in protonated and highly deuterated versions of the same molecule. Based on results from HCA II (Venters *et al.*, 1996), a single $^1H \rightarrow {}^2H$ substitution produces chemical shift changes of -0.29 ± 0.05, -0.13 ± 0.02, and -0.07 ± 0.02 ppm for a ^{13}C nucleus one, two, or three bonds away, respectively. Gardner *et al.* have measured average values for $^1\Delta\ ^{13}C(^2H)$ and $^2\Delta\ ^{13}C(^2H)$ of -0.25 and -0.1 ppm, respectively. These effects are additive, resulting in total shifts of over 1 ppm for ^{13}C nuclei at sites with many proximal deuterons such as is the case for sidechains of long aliphatic amino acids. Slightly smaller changes are typical for backbone nuclei, on the order of -0.3 ppm (^{15}N) and -0.5 ppm ($^{13}C\alpha$) for highly deuterated proteins dissolved in H_2O (Gardner and Kay, 1997; Garrett *et al.*, 1997; Venters *et al.*, 1996; Grzesiek *et al.*, 1993b; Kushlan and LeMaster, 1993b). The $^{13}C\alpha$ deuterium isotope shifts are weakly dependent on secondary structure (LeMaster *et al.*, 1994). In a recent study of the EIN protein, $^{13}C\alpha$ resonances were shifted upfield by an average of 0.50 ± 0.08 ppm for residues in α-helical regions of the protein compared with 0.44 ± 0.08 ppm for amino acids in β-strands (Garrett *et al.*, 1997). In contrast to the ^2H-isotope shift observed for aliphatic carbon resonances, no significant changes were observed between NH or carbonyl chemical shifts in a comparison between protonated and highly deuterated PLCC SH2 domains.

Given the additivity and only weak structural dependence of deuterium isotope effects, one can reliably transfer chemical shift assignments between fully protonated and perdeuterated molecules (Venters *et al.*, 1996). This facilitates the use of "secondary shift"-based identification of secondary structure elements (Wishart and Sykes, 1994) from the ^{13}C chemical shifts of deuterated proteins (Constantine *et al.*, 1997; Gardner *et al.*, 1997; Venters *et al.*, 1996). Note that transferability of carbon chemical shifts (i.e., the ability to calculate ^{13}C shifts in a protonated molecule from assignments obtained in a perdeuterated system and vice versa) is a prerequisite for combining data from deuterated and protonated proteins where chemical shifts obtained from a highly deuterated sample are used to assign NOE

cross-peaks recorded on a highly protonated molecule (Constantine *et al.*, 1997; Garrett *et al.*, 1997; Yu *et al.*, 1997; Venters *et al.*, 1996).

In the case of partially deuterated systems the presence of multiple deuterium-containing isotopomers at each site can significantly complicate spectra. Recall that in the case of the CT-HNCA experiment recorded on fractionally deuterated proteins, correlations involving $^{13}C\alpha$ sites that are protonated can be removed from spectra in a straightforward fashion by insertion of a single ^1H pulse. Signals from deuterated sites are unaffected by this pulse (Section 3.2). In the case of fractionally deuterated aliphatic sidechain sites the situation is somewhat more complex. Consider, for example, the high-resolution ^{13}C–^1H constant-time HSQC spectrum of a deuterated, methyl-protonated sample of the PLCC SH2 domain produced using pyruvate as a carbon source (Section 2.2.2) shown in Fig. 9a. Three peaks are observed for each Ala and Val methyl group, corresponding to the three possible proton-containing methyl isotopomers: CH_3, CH_2D, and CHD_2. Each methyl component is separated by deuterium isotope shifts of approximately 0.3 ppm for ^{13}C and 0.02 ppm for ^1H (Gardner *et al.*, 1997). A smaller number of isotopomers are observed for Met (two) and Thr (one), reflecting differences between these amino acids in the biosynthetic incorporation of protons from the protonated pyruvate carbon source.

Many of the multidimensional experiments that are used for assignment of chemical shifts and for measuring distance restraints are recorded with relatively short acquisition times in the indirect-detection dimensions (4–5 ms in carbon dimensions, for example), principally because of the lengthy acquisition times associated with collecting large (nD) data sets. In addition, in some applications acquisition times are constrained further by evolution involving passive homonuclear couplings. As such, these experiments are chiefly limited by poor digital resolution and cross-peaks from individual isotopomers are usually not resolved (Gardner *et al.*, 1997; Nietlispach *et al.*, 1996). However, in higher resolution spectra it is readily apparent that the deuterium isotopomers do significantly degrade spectral resolution, even in a well-dispersed spectrum recorded on a 12-kDa protein (Fig. 9a). As discussed in detail previously (Gardner *et al.*, 1997), the best solution to the problem is to eliminate all but CH_3 isotopomers during protein expression and in this regard Gardner and Kay have developed a strategy for producing highly deuterated, (Val, Leu, Ile $\delta 1$)-methyl-protonated proteins using appropriately labeled amino acids and amino acid precursors (Section 2.2.3). It is also possible to remove CH_2D and CHD_2 groups from ^{13}C–^1H correlation spectra using multipulse NMR methods although regrettably the spin alchemy employed does not restore the full complement of protons to the methyl groups that the biosynthetic approach described by Gardner and Kay (1997) provides. Nevertheless, the filtering schemes that have been used to suppress CH_2D and CHD_2 signals illustrate a number of important features regarding deuterium decoupling and purging of unwanted coherences that the reader may find of interest and with

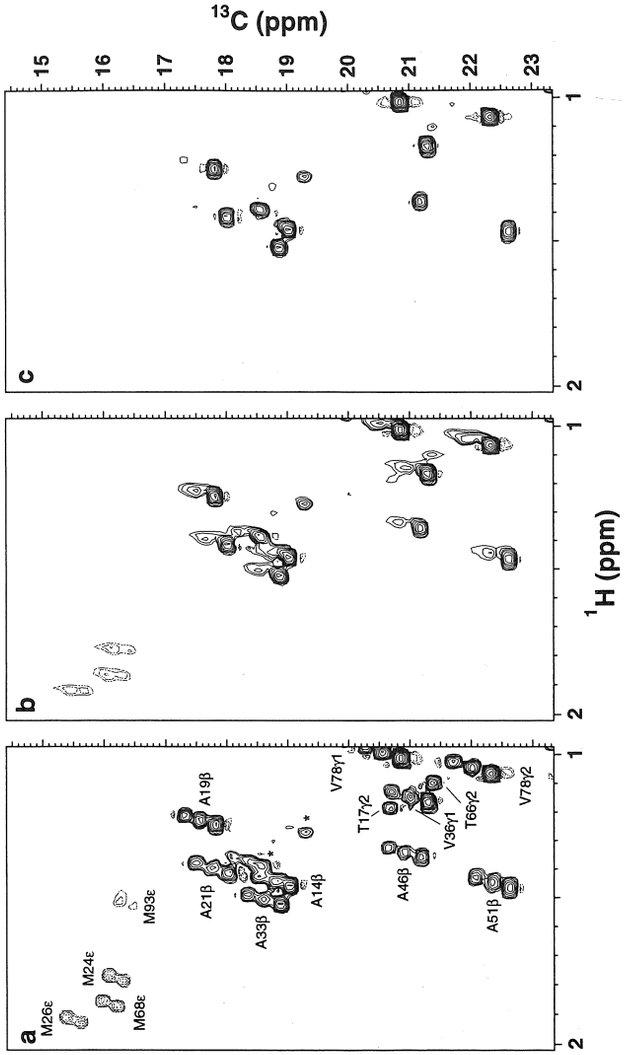

Figure 9. Removal of $^{13}CH_2D$ and $^{13}CHD_2$ cross-peaks in ^{13}C–^{1}H correlation spectra. All panels show a section of the methyl region from ^{13}C–^{1}H constant-time HSQC spectra recorded on an ^{15}N, ^{13}C, ^{2}H, ^{1}H-methyl (from ^{1}H-pyruvate)-labeled sample of the PLCC SH2 domain bound to a phosphotyrosine-containing peptide (Gardner *et al.*, 1997). (a) ^{2}H decoupling applied throughout the constant-time ^{13}C chemical shift evolution period (set to $1/J_{CC}$ ~ 28 ms) for maximum resolution of each methyl isotopomer (CH_3:CH_2D:CHD_2 from downfield to upfield for Ala and Val; CH_2D:CHD_2 for Met; CHD_2 for Thr). (b) Minimizing cross-peak intensities from deuterium-containing isotopomers by eliminating ^{2}H decoupling during ^{13}C chemical shift detection. (c) Elimination of cross-peaks from deuterium-containing isotopomers by removing deuterium decoupling as in (b) and application of the purging scheme described in the text. Reprinted with permission from Gardner *et al.* (1997).

this in mind a brief description of the approach that we have developed for retaining only CH_3 isotopomers is in order.

Sections 3.2 and 3.4 considered the importance of deuterium decoupling during the evolution of carbon magnetization. In the absence of decoupling deuterium spin flips mix carbon multiplet components associated with different deuterium spin states, leading to significant broadening and hence attenuation of cross-peaks. This feature can be put to good use in the separation of CH_3 isotopomers from CH_2D and CHD_2 groups in the present application. By eliminating deuterium decoupling during the constant-time delay period where carbon chemical shift is recorded, cross-peaks originating from deuterium-containing methyl groups are significantly attenuated, as illustrated in Fig. 9b. It is clear that in most experiments recorded on deuterated molecules where the idea is to maximize signal intensity from CD_n groups, deuterium decoupling is essential. To further reduce the intensity of cross-peaks from CH_2D methyl types, it is possible to actively purge magnetization from these groups. This is achieved by allowing carbon magnetization to evolve for a period of $1/(2J_{CH})$ from the start of the carbon constant-time period. At this point magnetization from CH_3, CH_2D, and CHD_2 groups is given by terms of the form, $C_{TR}I_{Z^i}I_{Z^j}$ $(i \neq j)$, $C_{TR}I_{Z^i}$, C_{TR}, respectively, where C_{TR} is transverse carbon magnetization and I_{Zk} refers to the z component of magnetization associated with methyl proton k. Application of an ^{1}H 90_x90_ϕ pulse pair where the phase ϕ is cycled $(x,-x)$ with no change in the receiver phase eliminates magnetization from CH_2D methyl groups. Additional purging of signals arising from partially deuterated methyls occurs by applying an ^{2}H purge (90°) pulse at a time of $1/(4J_{CD})$ after the start of the constant-time carbon evolution period, where J_{CD} is the one-bond ^{13}C–^{2}H coupling constant. As described in some detail previously (Gardner *et al.*, 1997), the outer components of a CD triplet evolve at a rate of $\pm 2\pi J_{CD}$, whereas in the case of a CD_2 spin system the lines closest to and farthest from the center line evolve with frequencies of $\pm 2\pi J_{CD}$ and $\pm 4\pi J_{CD}$, respectively (neglecting ^{2}H spin flips). Note that the central lines do not evolve. Given the range of frequencies over which different multiplet components evolve, it is not possible to eliminate all lines completely with a single purge pulse. In Fig. 9c a compromise delay of $1/(4J_{CD})$ has been employed and it is clear that excellent purging of CH_2D and CHD_2 groups has been achieved.

4. IMPACT OF DEUTERATION ON STRUCTURE DETERMINATION

4.1. Structure Determination of Perdeuterated Proteins

Current NMR solution structure determination methods rely heavily both on NOE-based interproton distance restraints and on scalar-coupling-based dihedral angle restraints (Wüthrich, 1986). The quality of any given structure is, of course,

heavily influenced by both the total number and the accuracy and precision of the input restraints (Hoogstraten and Markley, 1996; James, 1994; Zhao and Jardetzky, 1994; Clore *et al.*, 1993; Liu *et al.*, 1992). Because the number of restraints can vary significantly with deuteration levels and with the type of deuterium strategy employed, it is important to evaluate how each of the different deuteration approaches affects the quality of protein structures determined by NMR.

On a positive note the use of relatively high levels of deuteration (>75%) can improve the accuracy of NOE-derived interproton distance measurements, achieved largely through a reduction of spin diffusion. That is, by eliminating proton C that relays magnetization between protons A and B, the A–B separation can be measured more accurately. In addition, because the linewidths of the remaining protons in a deuterated molecule can be significantly narrowed (Section 1), overlap is reduced and, in the case of NH–NH cross-peaks, in particular, appreciable gains in sensitivity have been noted (Pachter *et al.*, 1992; LeMaster and Richards, 1988; Torchia *et al.*, 1988a,b). This leads to further improvements in the accuracy of distance measurements. Recently, 4D ^{15}N-, ^{15}N-edited NOESY experiments were developed (Grzesiek *et al.*, 1995; Venters *et al.*, 1995b) and data sets with high sensitivity and resolution can be recorded using samples of modest protein concentrations (1 mM). Deuteration also facilitates the use of longer NOE mixing times, allowing the measurement of larger distances than would be possible in protonated systems (Venters *et al.*, 1995b).

However, these benefits do come at a cost. Deuteration reduces the concentration of protons that would normally be available for providing NOE-based distance restraints, decreasing the total amount of structural information that can be used for analysis. In the most extreme case of a fully deuterated protein, the remaining protons derive exclusively from exchangeable sites such as amides and hydroxyls and only a subset of these will have sufficiently slow exchange rates and well-dispersed chemical shifts for analysis in NOESY experiments.

To investigate the impact of perdeuteration on the number of distance restraints that can be obtained from NOE experiments, we have used a data base of crystal structures solved to better than 2.5 Å that includes over 200 nonhomologous proteins (Heringa *et al.*, 1992) and tabulated the number of protons within 5 Å of each backbone amide proton. In the case of a fully protonated molecule, on average, 15.7 ± 2.0 protons are located within a 5-Å radius of each backbone NH. In contrast, only 2.5 ± 0.4 protons are within 5 Å of a backbone amide proton in the case of a fully deuterated molecule dissolved in H_2O. Two factors contribute to the sixfold reduction in the number of potential internuclear distance restraints involving backbone NHs that are available in a perdeuterated protein. Most obvious, the decrease in NOEs simply reflects the loss of protons that accompanies deuteration, as illustrated in Fig. 10 where a comparison of the distribution and numbers of protons within protonated and perdeuterated PLCC SH2 domains is provided. Perdeuteration leads to a fivefold reduction in the number of protons in this

molecule, from over 750 to approximately 60 sidechain and 90 backbone NHs. In addition, the spatial location of the majority of the remaining protons further lowers the number of possible NOE-based distance restraints. Many backbone and sidechain amide protons are involved in hydrogen-bonding networks in the core of secondary structure elements and are thus separated by distances of greater than 5 Å from protons on other α-helices or β-sheets. This is particularly problematic for α-helices, given the clustering of backbone NH protons in the centers of these structures (Gardner *et al.*, 1997).

Studies using either experimentally derived distance restraints or distances obtained on the basis of previously determined structures have established that backbone NH–NH distances of 5 Å or less will not, in general, be sufficient for calculating accurate global folds (Gardner *et al.*, 1997; Smith *et al.*, 1996; Venters *et al.*, 1995b). Structures generated in this manner typically have backbone heavy atom root-mean-square deviations (RMSD) on the order of 8 Å relative to reference structures. In addition, the precision of these folds is also quite poor, especially for proteins containing a high percentage of α-helix. It is noteworthy that Venters, Farmer, and co-workers have calculated well-defined global folds of HCA II using data sets generated from the known structure of the molecule where all backbone and sidechain NH NOEs within 7 Å are included (Venters *et al.*, 1995b). Unfortunately, with the current generation of spectrometers and with limitations imposed on sample concentration related to issues of solubility, aggregation, viscosity, or expense of production, it seems unlikely that large numbers of NH–NH distances beyond 5 Å will be observed for most systems. For example, only a small fraction (4%) of the possible NOEs connecting NH backbone protons separated by more than 5 Å were measured in a study of a highly deuterated PLCC SH2 domain (1.9 mM) in complex with target peptide (Gardner *et al.*, 1997). In general, therefore, additional NOE restraints are required to obtain overall folds of proteins.

4.2. Improving the Quality of Structures from Perdeuterated Systems: Additional Distance Restraints

As discussed above, the generation of accurate global folds of perdeuterated proteins requires that backbone NH–NH NOEs be supplemented by additional restraints. One obvious source of distance information derives from sidechain amide protons of Arg, Asn, and Gln. Note that these sidechain positions can, in principle, be fully protonated in a perdeuterated protein dissolved in H_2O. In addition to developing experiments for the site-specific assignment of sidechain amides, Farmer and Venters have also demonstrated the utility of sidechain NOEs in improving both the precision and accuracy of global fold determination from a limited NOE restraint set (Farmer and Venters, 1996). Figure 11a illustrates the distribution of sidechain NH protons from Arg, Asn, Gln, and Trp in the PLCC SH2 domain. Many of these protons are located in the interior of the molecule where

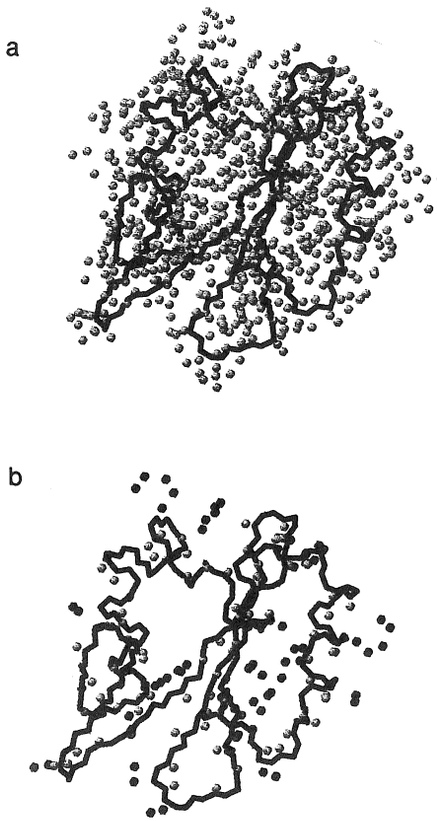

Figure 10. Effect of perdeuteration on the total number and distribution of protons within a protein. Protons from residues 10 to 100 in the PLCC SH2 domain are indicated by gray spheres while the protein N, Cα, C backbone is represented by a heavy black line (Pascal *et al.*, in preparation). (a) Fully protonated protein, containing a total of 756 protons. (b) Perdeuterated protein, containing 87 backbone amide and 62 sidechain amide protons on Arg, Asn, Gln, and Trp residues. The backbone and sidechain amide protons are represented by light and dark gray spheres, respectively. Figures were generated with the program MOLMOL (Koradi *et al.*, 1996).

they are sufficiently close to other NH protons to provide measurable distance restraints. However, a significant percentage are located on the exterior of the protein where they are likely prone to rapid exchange with solvent and poor chemical shift dispersion. Nevertheless, in the case of perdeuterated HCA II, Farmer and Venters were able to assign sidechain amide ^{1}H and ^{15}N chemical shifts for over 80% of the Asn and Gln residues and all of the Arg ε positions.

A second and more important source of additional NOE restraints derives from protonated methyl sites in otherwise highly deuterated proteins (Section 2.2). Several important factors enter into the choice of methyl groups as sites of protonation. First, the methyl region of ^{13}C–^{1}H correlation spectra is often reasonably well resolved and fast rotation about the methyl symmetry axis leads to narrow ^{13}C and ^{1}H linewidths, even in cases of large proteins (Kay *et al.*, 1992a). Analysis of the distribution of methyl-containing amino acids in proteins establishes that Ala, Val, Ile, and Leu are the most common residues in protein interiors and that Val and

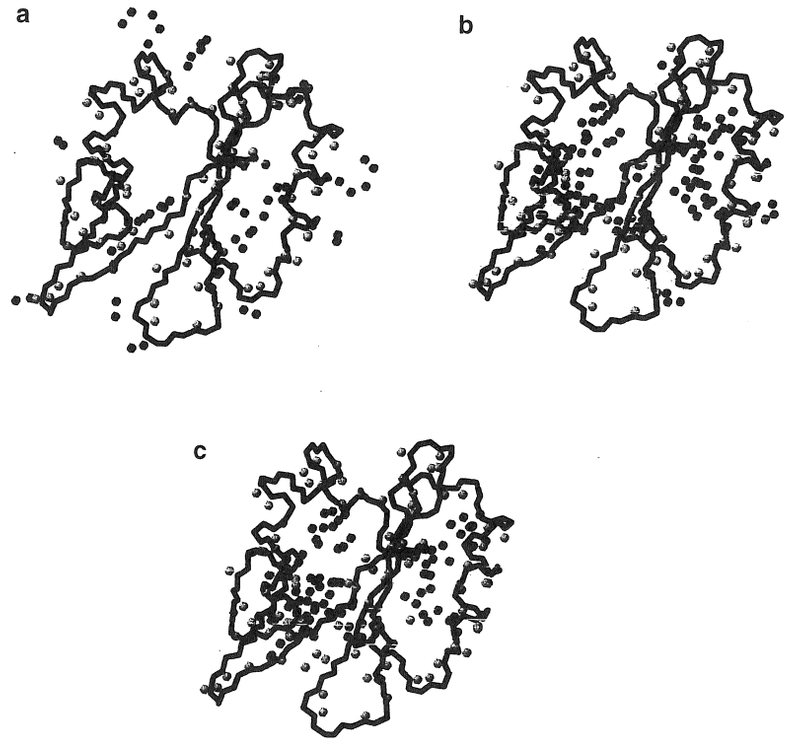

Figure 11. Distribution of sidechain protons in the PLCC SH2 domain obtained from different methods used to produce site-protonated, highly deuterated proteins. (a) Sidechain amide protons of Arg, Asn, Gln, and Trp available using any of the labeling strategies described in the text. (b) The 108 methyl protons of Ala, Val, Leu, and Ile (γ2 methyl only) produced using ^{1}H-pyruvate-based labeling (Rosen *et al.*, 1996). (c) Labeling scheme obtained using the method of Gardner and Kay based on the addition of [2,3-$^{2}H_2$]-^{15}N, ^{13}C-Val, and [3,3-$^{2}H_2$]-^{13}C 2-ketobutyrate to D_2O medium with ^{2}H,^{13}C-glucose as the carbon source. Ninety methyl protons are produced with this approach. In all figures, backbone amide protons are represented by light gray spheres while additional protons are drawn as dark gray spheres. Molecular graphics were generated with the program MOLMOL (Koradi *et al.*, 1996).

Leu are two of the three most abundant amino acids at molecular interfaces (Janin *et al.*, 1988). Therefore, protonated methyl groups are often within 5 Å of methyl or NH protons of other residues on different secondary structure elements. Figure 11b highlights the distribution of the methyl groups of Ala, Val, Ile (γ2 only), and Leu in the PLCC SH2 domain. Recall that this pattern of protonation is produced using D_2O-based media supplemented with ^{1}H-pyruvate (Section 2.2.2) (Rosen *et al.*, 1996). A similar distribution of methyl groups is observed for other patterns of site-specific protonation using deuterated, site-protonated or fully protonated forms

of these amino acids (Gardner and Kay, 1997; Metzler *et al.*, 1996b; Smith *et al.*, 1996). For example, Fig. 11c shows the aliphatic proton distribution in a sample generated by the procedure of Gardner and Kay (1997) where methyls from Val, Leu, and Ile ($\delta 1$ only) are protonated.

The utility of methyl site-specific protonation in providing additional distance restraints is readily appreciated by analyzing distances in a large set of nonhomologous proteins solved to high resolution by X-ray diffraction techniques (Heringa *et al.*, 1992). For example, an average of 5.1 ± 1.9 backbone amide protons and a total of 2.8 ± 1.5 Val γ, Ile $\delta 1$ ($i, i \neq j$) and Leu δ methyl groups are within 6 Å of a given Ile $\delta 1$ (j) methyl. NOEs between methyl protons in highly deuterated molecules where only the Val γ, Ile $\delta 1$, and Leu δ methyl groups are protonated (Section 2.2.3) involve residues with a median separation of 30 amino acids, as opposed to 2 and 3 for amide–amide and amide–methyl NOEs, respectively.

Given that intermethyl NOEs contain information constraining the location of residues that are so widely separated in the primary sequence, it is not surprising that they can significantly improve the quality of structures in relation to those calculated using distance restraints solely between backbone amide protons. Figure 12 illustrates this clearly by comparing several sets of structures of the PLCC SH2 domain generated using different subsets of NOE information. Figure 12a is a schematic representation of the secondary structure of this domain, highlighting the location of the methyl groups of Ala, Val, Ile ($\gamma 2$ only), and Leu at the interfaces between the central β-sheet and the two flanking α-helices. Figure 12b shows structures determined using only experimentally observed backbone NH–NH distances and loose (ϕ,ψ) dihedral angle restraints established from experiments performed on an ^{15}N, ^{13}C, ^{2}H (^{1}H-methyl Ala, Val, Ile($\gamma 2$), Leu) sample of this protein (Gardner *et al.*, 1997). Structures produced from such limited data are poorly defined as evidenced by the 3.5 Å RMSD of the 18 structures in Fig. 12b to the mean structure. More importantly, the experimentally determined structures have a different shape than the high-precision reference structure (bold line in Fig. 12b), because of the lack of long-range structural restraints and the use of a repulsive-only van der Waals potential. This distorts the overall fold, resulting in an RMSD of 7.7 Å between the experimental structures and the reference structure derived from data recorded on a fully protonated sample!

The accuracy and precision of the experimentally determined PLCC SH2 structures can be significantly improved by including distance restraints involving methyl groups obtained from 4D ^{13}C, ^{13}C-edited (Vuister *et al.*, 1993) and ^{13}C, ^{15}N-edited (Muhandiram *et al.*, 1993) NOESY experiments recorded on the ^{15}N, ^{13}C, ^{2}H, methyl-protonated sample described above. An additional 175 methyl–NH and methyl–methyl distance restraints are obtained from these two data sets and in combination with the NH–NH and dihedral angle restraints used to produce the structures of Fig. 12b generate the folds illustrated in Fig. 12c. The experimentally determined structures in Fig. 12c superimpose on the average and the reference

structures with backbone RMSD values of 2.4 and 3.1 Å, respectively. Note that the precision of the structures of Fig. 12c is considerably lower than for the reference structures determined from a fully protonated sample of the PLCC SH2 domain complexed with a 12-residue phosphopeptide (Fig. 12d). Similar conclusions regarding the importance of methyl NOEs have been noted in the case of simulations where tables of suitable interproton distances derived from crystal

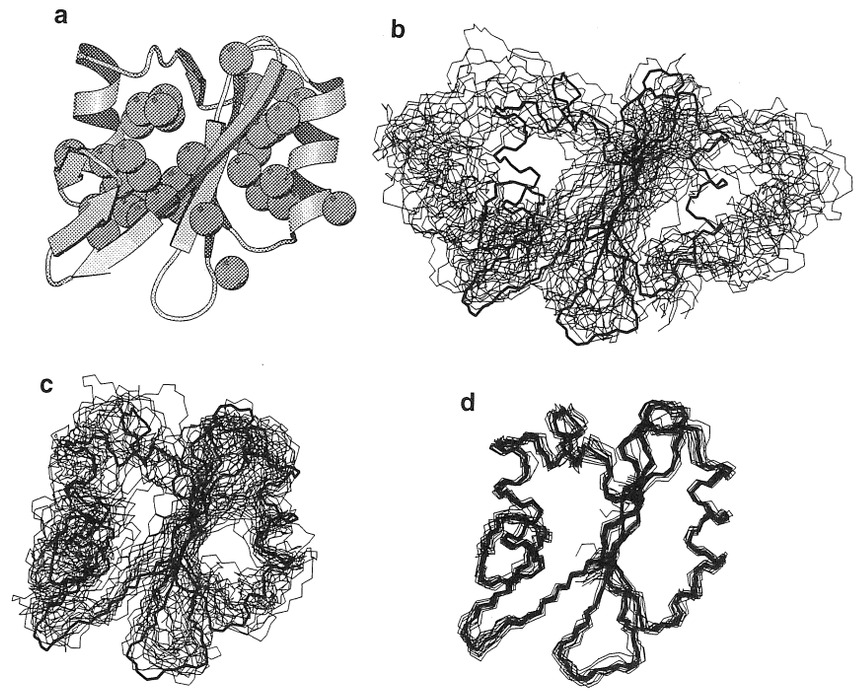

Figure 12. Structures of the PLCC SH2 domain obtained using different sets of distance restraints. (a) Schematic view showing ordered secondary structure elements identified by Pascal *et al.* (1994). Pyruvate-derived methyl groups are shown in a space-filling representation, highlighting their position between the central β-sheet and flanking α-helices. (b) Structures obtained on the basis of NH–NH NOEs and dihedral angle restraints established from $^{13}C\alpha$ and $^{13}C\beta$ chemical shifts (1.1 distance, 0.7 dihedral restraint/residue). (c) Structures generated by including methyl–methyl and NH–methyl restraints as well as the restraints in (b) (2.7 distance, 0.7 dihedral restraint/residue). (d) Reference structures, generated using an average of 16.0 distance and 1.7 dihedral angle restraints per residue, obtained from data recorded on a fully protonated sample (Pascal *et al.*, in preparation). Each bundle has 18 independently refined structures (thin lines) and is fit to the mean reference structure (thick line) using the backbone atoms of the secondary structure elements shown in (a). Panel (a) is drawn using MOLSCRIPT (Kraulis, 1991); all other panels were generated using MOLMOL (Koradi *et al.*, 1996). Reprinted with permission from Gardner *et al.* (1997).

structures are constructed and used to generate global folds of proteins (Gardner and Kay, 1997; Gardner *et al.*, 1997; Metzler *et al.*, 1996b; Smith *et al.*, 1996).

To date, most attention regarding potential sites of protonation in highly deuterated proteins has focused on methyl groups. From a structural perspective, aromatic residues are excellent candidates for protonation as well, as these amino acids are frequently important components of hydrophobic protein cores. However, the poor dispersion of aromatic ^{1}H and ^{13}C chemical shifts, the strong coupling between aromatic carbons, and the efficient transverse relaxation of aromatic ring spins complicate the use of these residues in a manner analogous to the use of methyl-containing amino acids described above. In addition, the large pseudoatom corrections required for aromatic-based distance restraints significantly lower the precision of the structural data available using these sites. In lieu of these problems, Smith *et al.* (1996) have suggested the use of ambiguously assigned NOEs (Nilges *et al.*, 1997; Nilges, 1995) involving protonated aromatic residues in determining the global folds of highly deuterated proteins.

4.3. Improving the Quality of Structures from Highly Deuterated Systems

4.3.1. NOE-Derived Distance Restraints

As of mid-1997, the largest monomeric protein structures that have been determined by NMR are of systems of approximately 30 kDa and include the 259-residue EIN protein (Garrett *et al.*, 1997) and the 245-residue ErmAm rRNA methyltransferase (Yu *et al.*, 1997). In both cases, highly (≥75%) deuterated samples were used for backbone and sidechain assignment as well as for the identification of proximal NH pairs from ^{15}N, ^{15}N-edited 4D NOESY experiments. The high sensitivity and resolution of this experiment, in particular, facilitate the rapid assignment of secondary structural elements. Despite the utility of deuteration in the assignment stages, the majority of interproton distances and all of the dihedral angle restraints used in structure determination were derived from experiments recorded on fully protonated samples.

Applications involving still larger proteins will likely be compromised by severe overlap and low signal intensity in spectra recorded on protonated molecules, necessitating the use of highly deuterated, amino-acid-protonated (Metzler *et al.*, 1996b; Smith *et al.*, 1996) (Section 2.2.1) or site-protonated (Gardner *et al.*, 1997, 1996; Rosen *et al.*, 1996) (Sections 2.2.2 and 2.2.3) proteins. However, as demonstrated so far (Gardner *et al.*, 1997; Metzler *et al.*, 1996b; Smith *et al.*, 1996), at best global folds of only moderate (2–3 Å) precision and accuracy can be obtained from a combination of methyl–methyl, methyl–NH, NH–NH NOEs and loose backbone dihedral angle restraints. Unfortunately, addition of sidechain NH–NH and sidechain NH–methyl restraints is unlikely to significantly improve the precision of structures beyond the limit of 2–3 Å. Clearly, more information is required

to improve the quality of structures derived from data collected exclusively on samples of highly deuterated proteins.

4.3.2. Dihedral Angle Restraints

As described briefly above, backbone dihedral angle restraints (*see* chapter 7) can be obtained indirectly from the chemical shifts of nuclei that are assigned during the initial stages of the structure determination process. The difference ($\Delta\delta$) between the chemical shifts of backbone proton and carbon nuclei from their random coil values is secondary structure dependent (Spera and Bax, 1991; Wishart *et al.*, 1991). In a highly deuterated, ^{13}C-labeled protein, the $\Delta\delta$ values calculated from $^{13}C\alpha$, $^{13}C\beta$, and ^{13}CO chemical shifts can be used to quickly and qualitatively identify whether a residue is in an α-helix or β-strand conformation using the chemical shift index (CSI) method (Wishart and Sykes, 1994) after suitable correction for deuterium isotope effects on ^{13}C chemical shifts (Section 3.6). Recently, Metzler, Farmer, Venters, and co-workers have suggested using a function of the form [$\Delta\delta$ ($^{13}C\alpha$) – $\Delta\delta$ ($^{13}C\beta$)] to identify secondary structural elements (Metzler *et al.*, 1996a, 1993; Venters *et al.*, 1996). A recent evaluation of the use of $^{13}C\alpha$ and $^{13}C\beta$ chemical shifts for secondary structure element identification based on a study of 14 proteins suggests that this approach can be used to correctly identify approximately 75% of α-helical and 50% of β-strand residues (Luginbühl *et al.*, 1995). However, in our experience the CSI method is a much more reliable indicator of secondary structure than this study suggests.

Chemical shift information can also be incorporated more quantitatively and directly into the structure determination process. For example, it is possible to perform direct structure refinement against $^{13}C\alpha$ and $^{13}C\beta$ chemical shifts (Kuszewski *et al.*, 1995b) or against (ϕ, ψ) dihedral angle restraints derived from $^{13}C\alpha$ shifts (Celda *et al.*, 1995). It may also be possible, in the case of partially protonated proteins, to refine against proton chemical shifts (Kuszewski *et al.*, 1995a). It is noteworthy that improvements in quantum mechanical calculations of chemical shifts as a function of (ϕ, ψ) will allow the use of tighter restraints than presently possible, significantly improving the quality of structures derived from sparse data sets (Le *et al.*, 1995; Oldfield, 1995).

The NOE-derived distance restraints and the loose (ϕ, ψ) restraints available from $^{13}C\alpha$ and $^{13}C\beta$ chemical shifts can be supplemented by additional dihedral angle restraints from measured coupling constants defining sidechain torsion angles. Recently, Konrat *et al.* (1997) and Bax and co-workers (Hu and Bax, 1997; Hu *et al.*, 1997) have developed triple-resonance pulse schemes for measuring χ_1 angles based on recording ^{15}N–$^{13}C\gamma$ and ^{13}CO–$^{13}C\gamma$ three-bond scalar couplings. Hennig *et al.* (1997) have described an experiment for measuring homonuclear three-bond couplings correlating $^{13}C\alpha$ and $^{13}C\delta$ spins in highly deuterated proteins, allowing determination of *trans*, *gauche*, or averaged $\chi 2$ rotameric states.

4.3.3. Bond Vector Restraints from Dipolar Couplings and Diffusion Anisotropy

A major shortcoming of NOE- and dihedral angle-based structural restraints is that they provide information only on local features such as short-range (≤5 Å) distances and angles between bonds that are proximal in sequence. Restraints between nuclei separated by distances in excess of 5 Å are difficult to obtain. In many cases, macromolecules consist of discrete domains or other structural elements separated by distances that are longer than those that can be measured using NOE methods. Recently a number of approaches have been described that address this limitation by providing restraints describing the relative orientation of domains in a manner that is independent of the distance between these modules (long range order).

One method for measuring long-range order in macromolecules is based on the well-known result that molecules with anisotropic magnetic susceptibilities will orient in an external magnetic field, B_o, with the degree of orientation a function of B_o^2 (Bastiaan *et al.*, 1987). Thus, the dipolar interaction between two spins, which in the high-field limit scales as $(3\cos^2\theta - 1)$ where θ is the angle between the vector joining these spins and B_o, no longer averages to zero (Tolman *et al.*, 1995). As a result, small residual splittings are observed. In the case of an axially symmetric susceptibility, these splittings depend on B_o^2, the size of the susceptibility anisotropy, and the angle between the dipole vector and the unique axis of the molecular susceptibility tensor. It is clear that the size of these splittings will be largest in molecules with large anisotropic magnetic susceptibility tensors including proteins with paramagnetic centers (Tolman *et al.*, 1995) or duplex DNA where smaller contributions to the susceptibility from each base pair add coherently (Kung *et al.*, 1995).

Residual dipolar contributions (*see* Volume 17, chapter 8) to splittings of ^{15}N resonances of ^{15}N–NH spin pairs and ^{13}C resonances of ^{13}Cα–^{1}Hα pairs in a number of proteins and protein–DNA complexes have been measured (Tjandra and Bax, 1997; Tjandra *et al.*, 1997b, 1996; Tolman *et al.*, 1995). Because the measured splittings are comprised of a field-invariant scalar coupling term, a dynamic frequency shift contribution that can be calculated, and a dipolar term that scales quadratically with field, dipolar contributions are readily obtained from a field dependent study. Differences in ^{15}N–NH splittings of between 0 and approximately –0.2 Hz have been measured for ubiquitin from spectra recorded at 600 and 360 MHz (Tjandra *et al.*, 1996). In contrast, dipolar couplings ranging from 1 to –5 Hz have been measured at 750 MHz in the case of the paramagnetic protein cyanometmyoglobin (Tolman *et al.*, 1995). The orientational dependence of the dipolar couplings with respect to the components of the susceptibility tensor can be exploited in structure refinement. In this regard a pseudoenergy potential has recently been developed for direct refinement against observed dipolar couplings during restrained molecular dynamics calculations and used in the structure determination of a GATA-1/DNA complex (Tjandra *et al.*, 1997b).

A second approach for obtaining long-range order in macromolecules is based on the measurement of ^{15}N relaxation times, T_1 and T_2. In the case of an isotropically tumbling molecule without internal motions, the ^{15}N T_1/T_2 ratio is uniform. In contrast, for a molecule with an axially symmetric diffusion tensor the T_1/T_2 ratio is a function of the angle between the N–NH bond vector and the unique axis of the diffusion tensor. In cases where the diffusion tensor is axially symmetric, therefore, it is possible to measure the orientation of each amide bond vector with respect to the diffusion frame and to use this information as an additional structural restraint, in an analogous manner to the use of dipolar couplings described above. Tjandra *et al.* (1997a) have shown that in the case of EIN ($D_{//} / D_{\perp} \sim 2$, where $D_{//}$ and $D_{\perp}$ are the parallel and perpendicular components of the diffusion tensor), ^{15}N T_1/T_2 data are important in defining the relative orientation of the two domains in the molecule.

4.3.4. Other Structural Information

In addition to the experiments described above, studies involving deuterium exchange (Wüthrich, 1986), paramagnetic perturbation of either chemical shifts (Guiles *et al.*, 1996; Gochin and Roder, 1995) and/or relaxation rates (Gillespie and Shortle, 1997; Kosen *et al.*, 1986), and chemical cross-linking (Das and Fox, 1979) can also provide useful distance restraints. Further information can be obtained from statistical analyses of data bases of previously determined protein structures. Residue-dependent preferences of various structural parameters, such as the values of backbone and sidechain dihedral angles or distances between pairwise combinations of amino acid residues, have been quantified and tables of these preferences converted into "knowledge-based" potentials of mean force to provide an energy scale to assign to values of these distances or dihedral angles (Jernigan and Bahar, 1996; Sippl, 1995). Such knowledge-based potentials have been used in a wide variety of applications, including error detection in experimentally determined structures, refinement of protein structures in combination with experimentally determined restraints (Kuszewski *et al.*, 1997, 1996; Skolnick *et al.*, 1997; Aszódi *et al.*, 1995), and *ab initio* structure prediction. One major advantage of knowledge-based potentials lies in their representation of structural information that is dependent on the entire range of molecular forces, including solvation effects. These potentials are thus better able to discriminate between favorable and unfavorable protein conformations than the commonly utilized potentials for van der Waals interactions. This, in turn, results in more efficient searches of conformational space and the generation of final structures with improved packing (Kuszewski *et al.*, 1996). A number of recent applications involving the use of knowledge-based dihedral angle potentials in structure calculations include studies of a specific

GAGA factor–DNA complex (Omichinski *et al.*, 1997) and the EIN protein (Garrett *et al.*, 1997).

In combination, the use of NOE and dihedral angle restraints, chemical shift deviations from random coil values, dipolar couplings, and protein structure data bases, will facilitate structure determination of higher molecular weight proteins using ^{2}H-based strategies with improved precision and accuracy.

5. USE OF DEUTERATION TO STUDY PROTEIN DYNAMICS

NMR spectroscopy can provide a wealth of information about molecular dynamics extending over a wide range of motional time scales. Studies to date have focused mostly on backbone dynamics, largely through measurement of backbone ^{15}N relaxation properties in uniformly ^{15}N labeled proteins (Nicholson *et al.*, 1996; Palmer, 1993). An attractive feature of backbone ^{15}N relaxation studies relates to the fact that the data can be easily analyzed. For example, the relaxation of a two-spin ^{15}N–NH spin pair can be described simply in terms of the ^{15}N–NH dipolar interaction and to a smaller extent by the ^{15}N chemical shift anisotropy (Kay *et al.*, 1989). Although interference between these two relaxation mechanisms does occur, methods have been developed that can effectively remove this complication (Kay *et al.*, 1992c; Palmer *et al.*, 1992).

The situation is, in general, more complex for the study of motional properties of sidechains. Although the use of carbon relaxation to probe sidechain dynamics appears to be an obvious approach, ^{13}C relaxation methods are not without some rather significant problems. First, most sidechain positions are of either the CH_2 or CH_3 variety and cross correlation between ^{13}C–^{1}H dipolar interactions can be significant in these cases (Kay *et al.*, 1992a; Palmer *et al.*, 1991a). Although the interpretation of such effects provides powerful insight into molecular dynamics (Werbelow and Grant, 1977), several experiments must often be performed where the relaxation behavior of the individual multiplet components is monitored. In addition, relaxation contributions from neighboring spins can complicate the extraction of accurate dynamics parameters. Second, differential relaxation of multiplet components occurring during the course of the pulse sequences used to measure ^{13}C relaxation times results in the transfer of magnetization from ^{13}C to ^{1}H in a manner that may not reflect the equilibrium intensity of each carbon multiplet component. Although pulse sequences which minimize this effect in the case of methyl groups have been described (Kay *et al.*, 1992a), they do not eliminate the problem completely. Third, in the case of applications involving uniformly ^{13}C labeled samples, both scalar and dipolar ^{13}C–^{13}C couplings must be taken into account (Engelke and Rüterjans, 1995; Yamazaki *et al.*, 1994c). Although this problem is eliminated through the use of molecules in which only a select number

of sites are labeled, the information content available in such systems is, of course, much less.

A recent series of papers by LeMaster and Kushlan have addressed many of the abovementioned limitations in the use of ^{13}C spectroscopy to study sidechain dynamics (LeMaster and Kushlan, 1996; Kushlan and LeMaster, 1993a). Using a suitable strain of *E. coli* grown on medium containing either [2-^{13}C]-glycerol or [1,3-$^{13}C_2$]-glycerol, LeMaster and Kushlan have shown that it is possible to produce proteins in which isotopic enrichment is largely restricted to alternating carbon sites and in this manner eliminate the deleterious effects of carbon–carbon couplings. In addition, complications arising from the presence of more than one proton attached to a given ^{13}C spin are removed through the use of approximately 50% random fractional deuteration in concert with pulse schemes that select for ^{13}C–^{1}H two-spin spin systems. The method has been applied to investigate the dynamics of *E. coli* thioredoxin, a small protein of 108 residues (LeMaster and Kushlan, 1996).

To this point in the review all applications discussed have made use of deuteration simply as a method for removing proton spins, thereby improving the relaxation properties of the remaining NMR-active nuclei (Sections 2–4) or simplifying analysis of ^{13}C relaxation times in terms of molecular dynamics (Section 5). These deuterons can be thought of as passive participants in the experiments in that none of their spectroscopic properties are recorded. It is possible, however, to make use of fractionally deuterated protein samples in quite a different way than has been previously described to obtain information about protein dynamics. In this regard, it is noteworthy that ^{2}H NMR has enjoyed a rich history in the study of biomolecular motion through measurement of deuterium relaxation and line-shape parameters (Vold and Vold, 1991; Keniry *et al.*, 1983; Jelinski *et al.*, 1980; Seelig, 1977). Applications have largely focused on liquid-crystalline and solid-state samples (Keniry, 1989). The low sensitivity of ^{2}H direct detect spectra coupled with broad linewidths and poor chemical dispersion has, until recently, restricted the application of high-resolution solution-state ^{2}H NMR methods to a few relaxation studies of site-specifically deuterated proteins for estimate of molecular rotational correlation times (Schramm and Oldfield, 1983; Johnson *et al.*, 1989). However, the power of ^{2}H relaxation as a probe of molecular dynamics, largely the result of the fact that the relaxation is dominated by the well-understood quadrupolar interaction, has stimulated interest in developing solution-state-based methods for measuring ^{2}H relaxation rates that do not suffer from the problems mentioned above.

Recently, a triple-resonance method has been described for the measurement of ^{2}H spin relaxation times, T_1 and $T_{1\rho}$, in fractionally deuterated ^{15}N, ^{13}C labeled proteins (Muhandiram *et al.*, 1995). The idea is to select for methylene or methyl groups with only a single attached deuteron, allow relaxation of magnetization proportional to either $D_z(T_1)$ or $D_y(T_{1\rho})$ to proceed for a delay time, T, during the course of the experiment and encode this decay in cross-peak intensities measured

in ^{13}C–^{1}H constant-time correlation spectra. Thus, the approach makes use of a series of magnetization transfer steps in which signal originating on a sidechain (^{13}CHD, Yang *et al.*, 1998; $^{13}CH_2D$, Muhandiram *et al.*, 1995) proton is transferred to the attached carbon and subsequently to the deuteron bound to the same carbon. At this point the relaxation proceeds for a defined time, T, and the signal is subsequently returned to the originating proton for detection. The flow of magnetization during the course of the experiment can be represented by

$$^{1}H \xrightarrow{J_{CH}} {}^{13}C \xrightarrow{J_{CD}} {}^{2}H\,(T) \xrightarrow{J_{CD}} {}^{13}C\,(t_1) \xrightarrow{J_{CH}} {}^{1}H\,(t_2)$$

where the active couplings involved in each INEPT-based transfer are indicated above the arrows and t_1 and t_2 denote periods during which ^{13}C and ^{1}H chemical shifts are recorded. A set of 2D (^{13}C,^{1}H) correlation spectra are obtained where the time profile of the intensity of a cross-peak arising from a $^{13}CH_2D$ methyl, for example, is related to the relaxation time (T_1 or $T_{1\rho}$) of the attached deuteron. In practice, because of the magnetization transfer steps that are involved, the decay of operators of the form $I_zC_zD_z$ (T_1) or $I_zC_zD_y$ ($T_{1\rho}$) is measured during the relaxation time, T. T_1 and $T_{1\rho}$ values of pure deuterium magnetization can be obtained by recording an additional experiment in which the decay of the two-spin order, I_zC_z, is measured and subtracting this rate from the decay rates of $I_zC_zD_z$ and $I_zC_zD_y$ according to

$$1/T_1(D_z) = 1/T_1(I_zC_zD_z) - 1/T_1(I_zC_z)$$

$$1/T_{1\rho}(D_y) = 1/T_{1\rho}(I_zC_zD_y) - 1/T_1(I_zC_z).$$

Cross correlation between the many different relaxation mechanisms that could potentially complicate the decay of the triple spin terms described above has been examined in detail and shown not to contribute in a measurable way to the decay of the magnetization (Yang and Kay, 1996).

The deuterium relaxation methods described above have been applied to study the sidechain dynamics of the PLCC SH2 domain, in both the presence and absence of target peptide (Kay *et al.*, 1996). Remarkably, certain residues in the hydrophobic binding region of this SH2 domain which are important for the specificity of its interaction with peptide, are highly mobile in both peptide free and complexed states. A comparison of the dynamics of the PLCC SH2 domain with the amino-terminal SH2 domain from the Syp phosphatase has provided insight into the origin of the very different peptide-binding properties of these two highly homologous structures (Kay *et al.*, 1998).

Recently, Pervushin *et al.* (1997) have described 2D heteronuclear experiments for measuring transverse and longitudinal ^{2}H relaxation rates in ^{15}NHD groups (Asn and Gln) in uniformly ^{15}N labeled proteins. Samples are dissolved in a 1:1 mixture of H_2O/D_2O to give maximal concentrations of ^{15}NHD groups with deuteration at

either E or Z positions. These pulse sequences are closely related to the ^{13}C–^{2}H relaxation experiments described above. Interestingly, because the direction of the bond connecting the amide nitrogen and the $^{2}H^{Z}$ deuteron is nearly parallel to the Cβ–Cγ or Cγ–Cδ bond in Asn and Gln, respectively, rotation about χ_2 (Asn) or χ_3 (Gln) affects the transverse relaxation of $^{2}H^{Z}$ much less than $^{2}H^{E}$. Thus, the relaxation rates for $^{2}H^{Z}$ are predicted to be larger than for $^{2}H^{E}$; this has been observed in relaxation studies of the 70-residue *ftz* (fushi-tarazu) homeodomain and its complex with a 14-base-pair DNA.

6. CONCLUDING REMARKS

The present review has highlighted many of the important current advances in the use of deuteration for both structural and dynamics studies of proteins and protein complexes. Outstanding areas of investigation include the further development of labeling schemes for site-specific incorporation of protons in highly deuterated proteins, new pulse sequence methodology that is customized for the labeling methods that will be introduced, and the design of new classes of experiments that provide structural parameters complementary to the existing NOE- and scalar-coupling-based classes of restraints. It is also clear that further increases in magnetic fields, resulting in gains in dispersion and sensitivity for multidimensional NMR applications, and future improvements in spectrometer hardware will also impact significantly on the scope of problems that can be studied. The future promises to be exciting indeed.

ACKNOWLEDGMENTS. The authors thank Julie Forman-Kay (Hospital for Sick Children, Toronto) for helpful discussions and a critical reading of the manuscript and Drs. Dan Garrett (NIH) and Steve Fesik (Abbott Laboratories) for providing preprints. This work was supported by a grant from the Medical Research Council of Canada. K.H.G. gratefully acknowledges a postdoctoral fellowship from the Helen Hay Whitney Foundation.

REFERENCES

Agback, P., Maltseva, T. V., Yamakage, S.-I., Nilsson, F. P. R., Földesi, A., and Chattopadhyaya, J., 1994, *Nucl. Acids Res.* **22:**1404–1412.

Allerhand, A., Doddrell, D., Glushko, V., Cochran, D. W., Wenkert, E., Lawson, P. J., and Gurd, F. R. N., 1971, *J. Am. Chem. Soc.* **93:**544–546.

Anglister, J., 1990, *Q. Rev. Biophys.* **23:**175–203.

Arrowsmith, C. H., Pachter, R., Altman, R. B., Iyer, S. B., and Jardetzky, O., 1990a, *Biochemistry* **29:**6332–6341.

Arrowsmith, C. H., Treat-Clemons, L., Szilágyi, L., Pachter, R., and Jardetzky, O., 1990b, *Makromol. Chem. Macromol. Symp.* **34:**33–46.

Aszódi, A., Gradwell, M. J., and Taylor, W. R., 1995, *J. Mol. Biol.* **251:**308–326.
Bastiaan, E. W., Maclean, C., Van Zijl, P. C. M., and Bothner-By, A. A., 1987, *Annu. Rep. NMR Spectrosc.* **19:**35–77.
Batey, R. T., Cloutier, N., Mao, H., and Williamson, J. R., 1996, *Nucl. Acids Res.* **24:**4836–4837.
Bax, A., 1994, *Curr. Opin. Struct. Biol.* **4:**738–744.
Bax, A., De Jong, D. E., Mehlkopf, A. F., and Smidt, J., 1980, *Chem. Phys. Lett.* **69:**567–570.
Boyd, J., Soffe, N., John, B., Plant, D., and Hurd, R., 1992, *J. Magn. Reson.* **98:**660–664.
Brodin, P., Drakenberg, T., Thulin, E., Forsén, S., and Grundström, T., 1989, *Protein Eng.* **2:**353–358.
Browne, D. T., Kenyon, G. L., Packer, E. L., Sternlicht, H., and Wilson, D. M., 1973, *J. Am. Chem. Soc.* **95:**1316–1323.
Cavanagh, J., and Rance, M., 1988, *J. Magn. Reson.* **88:**72–85.
Celda, B., Biamonti, C., Arnau, M. J., Tejero, R., and Montelione, G. T., 1995, *J. Biomol. NMR* **5:**161–172.
Clore, G. M., and Gronenborn, A. M., 1994, *Methods Enzymol.* **239:**349–363.
Clore, G. M., Robien, M. A., and Gronenborn, A. M., 1993, *J. Mol. Biol.* **231:**82–102.
Constantine, K. L., Mueller, L., Goldfarb, V., Wittekind, M., Metzler, W. J., Yanuchas, J. J., Robertson, J. G., Malley, M. F., Friedrichs, M. S., and Farmer, B. T., II, 1997, *J. Mol. Biol.* **267:**1223–1246.
Crespi, H. L., and Katz, J. J., 1969, *Nature* **224:**560–562.
Crespi, H. L., Rosenberg, R. M., and Katz, J. J., 1968, *Science* **161:**795–796.
Das, M., and Fox, C. F., 1979, *Annu. Rev. Biophys. Bioeng.* **8:**165–193.
Davis, A. L., Keeler, J., Laue, E. D., and Moskau, D., 1992, *J. Magn. Reson.* **98:**207–216.
Dötsch, V., Matsuo, H., and Wagner, G., 1996, *J. Magn. Reson. B* **112:**95–100.
Eisenstein, E., 1991, *J. Biol. Chem.* **266:**5801–5807.
Engelke, J. and Rüterjans, H., 1995, *J. Biomol. NMR* **5:**173–182.
Farmer, B. T., II, and Venters, R. A., 1995, *J. Am. Chem. Soc.* **117:**4187–4188.
Farmer, B. T., II, and Venters, R. A., 1996, *J. Biomol. NMR* **7:**59–71.
Földesi, A., Yamakage, S.-I., Nilsson, F. P. R., Maltseva, T. V., and Chattopadhyaya, J., 1996, *Nucl. Acids Res.* **24:**1187–1194.
Galimov, E. M., 1985, *The Biological Fractionation of Isotopes*, Academic Press, Orlando.
Gardner, K. H., and Kay, L. E., 1997, *J. Am. Chem. Soc.* **119:**7599–7600.
Gardner, K. H., Konrat, R., Rosen, M. K., and Kay, L. E., 1996, *J. Biomol. NMR* **8:**351–356.
Gardner, K. H., Rosen, M. K., and Kay, L. E., 1997, *Biochemistry* **36:**1389–1401.
Garrett, D. S., Seok, Y., Liao, D., Peterkofsky, A., Gronenborn, A. M., and Clore, G. M., 1997, *Biochemistry* **36:**2517–2530.
Gillespie, J. R., and Shortle, D., 1997, *J. Mol. Biol.* **268:**158–169.
Gochin, M., and Roder, H., 1995, *Protein Sci.* **4:**296–305.
Griffey, R. H., and Redfield, A. G., 1987, *Q. Rev. Biophys.* **19:**51–82.
Grzesiek, S., and Bax, A., 1992, *J. Magn. Reson.* **96:**432–440.
Grzesiek, S., and Bax, A., 1993, *J. Am. Chem. Soc.* **115:**12593–12594.
Grzesiek, S., and Bax, A., 1994, *J. Am. Chem. Soc.* **116:**10196–10201.
Grzesiek, S., and Bax, A., 1995, *J. Biomol. NMR* **6:**335–339.
Grzesiek, S., Anglister, J., and Bax, A., 1993a, *J. Magn. Reson. B* **101:**114–119.
Grzesiek, S., Anglister, J., Ren, H., and Bax, A., 1993b, *J. Am. Chem. Soc.* **115:**4369–4370.
Grzesiek, S., Wingfield, P., Stahl, S., Kaufman, J. D., and Bax, A., 1995, *J. Am. Chem. Soc.* **117:**9594–9595.
Guiles, R. D., Sarma, S., DiGate, R. J., Banville, D., Basus, V. J., Kuntz, I. D., and Waskell, L., 1996, *Nature Struct. Biol.* **3:**333–339.
Hansen, A. P., Petros, A. M., Mazar, A. P., Pederson, T. M., Rueter, A., and Fesik, S. W., 1992, *Biochemistry* **31:**12713–12718.
Hansen, P. E., 1988, *Prog. NMR Spectrosc.* **20:**207–255.

Hennig, M., Ott, D., Schulte, P., Löwe, R., Krebs, J., Vorherr, T., Bermel, W., Schwalbe, H. and Griesinger, C., 1997, *J. Am. Chem. Soc.* **119:**5055–5056.
Heringa, J., Sommerfeldt, H., Higgins, D., and Argos, P., 1992, *CABIOS* **8:**599–600.
Homer, R. J., Kim, M. S., and LeMaster, D. M., 1993, *Anal. Biochem.* **215:**211–215.
Hoogstraten, C. G., and Markley, J. L., 1996, *J. Mol. Biol.* **258:**334–348.
Hsu, V. L., and Armitage, I. M., 1992, *Biochemistry* **31:**12778–12784.
Hu, J.-S., and Bax, A., 1997, *J. Am. Chem. Soc.* **119:**6360–6368.
Hu, J.-S., Grzesiek, S., and Bax, A., 1997, *J. Am. Chem. Soc.* **119:**1803–1804.
Ikegami, T., Sato, S., Wälchli, M., Kyogoku, Y. and Shirakawa, M., 1997, *J. Magn. Reson.* **124:**214–217.
Ikura, M., Kay, L. E., and Bax, A., 1990, *Biochemistry* **29:**4659–4667.
James, T., 1994, *Methods Enzymol.* **239:**416–439.
Janin, J., Miller, S., and Chothia, C., 1988, *J. Mol. Biol.* **204:**155–164.
Jelinski, L. W., Sullivan, C. E., and Torchia, D. A., 1980, *Nature* **284:**531–534.
Jernigan, R. L., and Bahar, I., 1996, *Curr. Opin. Struct. Biol.* **6:**195–209.
Johnson, R. D., La Mar, G. N., Smith, K. M., Parish, D. W., and Langry, K. C., 1989, *J. Am. Chem. Soc.* **111:**481–485.
Kalbitzer, H. R., Leberman, R., and Wittinghofer, A., 1985, *FEBS Lett.* **180:**40–42.
Katz, J. J., and Crespi, H. L., 1966, *Science* **151:**1187–1194.
Kay, L. E., 1995a, *Curr. Opin. Struct. Biol.* **5:**674–681.
Kay, L. E., 1995b, *Prog. Biophys. Mol. Biol.* **63**:277–299.
Kay, L. E., Torchia, D. A., and Bax, A., 1989, *Biochemistry* **28:**8972–8979.
Kay, L. E., Ikura, M., Tschudin, R., and Bax, A., 1990, *J. Magn. Reson.* **89:**496–514.
Kay, L. E., Bull, T., Nicholson, L. K., Griesinger, C., Schwalbe, H., Bax, A., and Torchia, D., 1992a, *J. Magn. Reson.* **100:**538–558.
Kay, L. E., Keifer, P., and Saarinen, T., 1992b, *J. Am. Chem. Soc.* **114:**10663–10665.
Kay, L. E., Nicholson, L. K., Delaglio, F., Bax, A., and Torchia, D. A., 1992c, *J. Magn. Reson.* **97:**359–375.
Kay, L. E., Xu, G. Y., and Yamazaki, T., 1994, *J. Magn. Reson. A* **109:**129–133.
Kay, L. E., Muhandiram, D. R., Farrow, N. A., Aubin, Y., and Forman-Kay, J. D., 1996, *Biochemistry* **35**:362–368.
Kay, L. E., Muhandiram, D. R., Wolf G., Shoelson, S. E., and Forman-Kay, J. D., 1998, *Nat. Struct. Biol.* **5:**156–163.
Keeler, J., Clowes, R. T., Davis, A. L., and Laue, E. D., 1994, *Methods Enzymol.* **239**:145–207.
Keniry, M. A., 1989, *Methods Enzymol.* **176:**376–386.
Keniry, M. A., Rothgeb, T. M., Smith, R. L., Gutowsky, H. S., and Oldfield, E., 1983, *Biochemistry* **22:**1917–1926.
Konrat, R., Muhandiram, D. R., Farrow, N. A., and Kay, L. E., 1997, *J. Biomol. NMR* **9:**409–422.
Koradi, R., Billeter, M., and Wüthrich, K., 1996, *J. Mol. Graphics* **14:**51–55.
Kosen, P. A., Scheck, R. M., Nadevi, H., Basus, V. J., Manogaran, S., Schmidt, P. G., Oppenheimer, N. J., and Kuntz, I. D., 1986, *Biochemistry* **25:**2356–2364.
Kraulis, P. J., 1991, *J. Appl. Crystallogr.* **24:**946–950.
Kung, H. C., Wang, K. Y., Goljer, I., and Bolton, P. H., 1995, *J. Magn. Reson. B* **109:**323–325.
Kushlan, D. M., and LeMaster, D. M., 1993a, *J. Am. Chem. Soc.* **115:**11026–11027.
Kushlan, D. M., and LeMaster, D. M., 1993b, *J. Biomol. NMR* **3:**701–708.
Kuszewski, J., Gronenborn, A. M., and Clore, G. M., 1995a, *J. Magn. Reson. B* **107:**293–297.
Kuszewski, J., Qin, J., Gronenborn, A. M., and Clore, G. M., 1995b, *J. Magn. Reson. B* **106:**92–96.
Kuszewski, J., Gronenborn, A. M., and Clore, G. M., 1996, *Protein Sci.* **5:**1067–1080.
Kuszewski, J., Clore, G. M., and Gronenborn, A. M., 1997, *J. Magn. Reson.* **125:**171–177.
Le, H., Pearson, J. G., de Dios, A. C., and Oldfield, E., 1995, *J. Am. Chem. Soc.* **117:**3800–3807.
LeMaster, D. M., 1989, *Methods Enzymol.* **177:**23–43.

LeMaster, D. M., 1990, *Q. Rev. Biophys.* **23:**133–173.
LeMaster, D. M., 1994, *Prog. NMR Spectrosc.* **26:**371–419.
LeMaster, D. M., 1997, *J. Biomol. NMR* **9:**79–93.
LeMaster, D. M., and Kushlan, D. M., 1996, *J. Am. Chem. Soc.* **118:**9255–9264.
LeMaster, D. M., and Richards, F. M., 1988, *Biochemistry* **27:**142–150.
LeMaster, D. M., LaIuppa, J. C., and Kushlan, D. M., 1994, *J. Biomol. NMR* **4:**863–870.
Liu, Y., Zhao, D., Altman, R., and Jardetzky, O., 1992, *J. Biomol. NMR* **2:**373–388.
Logan, T. M., Olejniczak, E. T., Xu, R. X., and Fesik, S. W., 1992, *FEBS Lett.* **314:**413–418.
Logan, T. M., Olejniczak, E. T., Xu, R. X., and Fesik, S. W., 1993, *J. Biomol. NMR* **3:**225–231.
London, R. E., LeMaster, D. M., and Werbelow, L. G., 1994, *J. Am. Chem. Soc.* **116:**8400–8401.
Luginbühl, P., Szyperski, T., and Wüthrich, K., 1995, *J. Magn. Reson. B* **109:**229–233.
Markley, J. L., Putter, I., and Jardetzky, O., 1968, *Science* **161:**1249–1251.
Markus, M. A., Kayie, K. T., Matsudaira, P., and Wagner, G., 1994, *J. Magn. Reson. B* **105:**192–195.
Martin, M. L., and Martin, G. J., 1990, in *NMR Basic Principles and Progress*, Vol. 23, eds., Springer-Verlag, Berlin, pp. 1–61.
Matsuo, H., Kupce, E., Li, H., and Wagner, G., 1996a, *J. Magn. Reson. B* **111:**194–198.
Matsuo, H., Li, H., and Wagner, G., 1996b, *J. Magn. Reson. B.* **110:**112–115.
Maudsley, A. A., Wokaun, A., and Ernst, R. R., 1978, *Chem. Phys. Lett.* **55:**9–14.
McIntosh, L. P., and Dahlquist, F. W., 1990, *Q. Rev. Biophys.* **23:**1–38.
Metzler, W. J., Constantine, K. L., Friedrichs, M. S., Bell, A. J., Ernst, E. G., Lavoie, T. B., and Mueller, L., 1993, *Biochemistry* **32:**13818–13829.
Metzler, W. J., Leiting, B., Pryor, K., Mueller, L., and Farmer, B. T., II, 1996a, *Biochemistry* **35:**6201–6211.
Metzler, W. J., Wittekind, M., Goldfarb, V., Mueller, L., and Farmer, B. T., II, 1996b, *J. Am. Chem. Soc.* **118:**6800–6801.
Montelione, G. T., Lyons, B. A., Emerson, D. S., and Tashiro, M., 1992, *J. Am. Chem. Soc.* **114:**10974–10975.
Moore, P. B., 1979, *Methods Enzymol.* **59:**639–655.
Muhandiram, D. R., and Kay, L. E., 1994, *J. Magn. Reson. B* **103:**203–216.
Muhandiram, D. R., Xu, G. Y., and Kay, L. E., 1993, *J. Biomol. NMR* **3:**463–470.
Muhandiram, D. R., Yamazaki, T., Sykes, B. D., and Kay, L. E., 1995, *J. Am. Chem. Soc.* **117:**11536–11544.
Murali, N., and Rao, B. D. N., 1996, *J. Magn. Reson. A* **118:**202–213.
Nicholson, L. K., Kay, L. E. and Torchia, D. A., 1996, in *NMR Spectroscopy and Its Application to Biomedical Research* (S. K. Sarkar, ed.), Elsevier, Amsterdam, pp. 241–280.
Nietlispach, D., Clowes, R. T., Broadhurst, R. W., Ito, Y., Keeler, J., Kelly, M., Ashurst, J., Oschkinat, H., Domaille, P. J., and Laue, E. D., 1996, *J. Am. Chem. Soc.* **118:**407–415.
Nilges, M., 1995, *J. Mol. Biol.* **245:**645–660.
Nilges, M., Macias, M. J., O'Donoghue, S. I., and Oschkinat, H., 1997, *J. Mol. Biol.* **269:**408–422.
Oda, Y., Nakamura, H., Yamazaki, T., Nagayama, K., Yoshida, M., Kanaya, S., and Ikehara, M., 1992, *J. Biomol. NMR* **2:**137–147.
Oldfield, E., 1995, *J. Biomol. NMR* **5:**217–225.
Omichinski, J. G., Pedone, P. V., Felsenfeld, G., Gronenborn, A. M., and Clore, G. M., 1997, *Nature Struct. Biol.* **4:**122–132.
Ono, A., Makita, T., Tate, S., Kawashima, E., Ishido, Y., and Kainosho, M., 1996, *Magn. Reson. Chem.* **34:**S40–S46.
Pachter, R., Arrowsmith, C. H., and Jardetzky, O., 1992, *J. Biomol. NMR* **2:**183–194.
Palmer, A. G., III, 1993, *Curr. Opin. Biotechnol.* **4:**385–391.
Palmer, A. G., III, Wright, P. E., and Rance, M., 1991a, *Chem. Phys. Lett.* **185:**41–46.
Palmer, A. G., III, Cavanagh, J., Wright, P. E., and Rance, M., 1991b, *J. Magn. Reson.* **93:**151–170.

Palmer, A. G., III, Skelton, N. J., Chazin, W. J., Wright, P. E., and Rance, M., 1992, *Mol. Phys.* **75:**699–711.
Pascal, S. M., Singer, A. U., Gish, G., Yamazaki, T., Shoelson, S. E., Pawson, T., Kay, L. E., and Forman-Kay, J. D., 1994, *Cell* **77:**461–472.
Pascal, S. M., Singer, A. U., Kay, L. E., and Forman-Kay, J. D., 1997, in preparation.
Pervushin, K., Wider, G., and Wüthrich, K., 1997, *J. Am. Chem. Soc.* **119:**3842–3843.
Reisman, J., Jariel-Encontre, I., Hsu, V. L., Parello, J., Guiduschek, E. P., and Kearns, D. R., 1991, *J. Am. Chem. Soc.* **113:**2787–2789.
Reisman, J. M., Hsu, V. L., Jariel-Encontre, I., Lecou, C., Sayre, M. H., Kearns, D. R., and Parello, J., 1993, *Eur. J. Biochem.* **213:**865–873.
Rosen, M. K., Gardner, K. H., Willis, R. C., Parris, W. E., Pawson, T., and Kay, L. E., 1996, *J. Mol. Biol.* **263:**627–636.
Santoro, J., and King, G. C., 1992, *J. Magn. Reson.* **97:**202–207.
Sattler, M., and Fesik, S. W., 1996, *Structure* **4:**1245–1249.
Schleucher, J., Sattler, M., and Griesinger, C., 1993, *Angew. Chem. Int. Ed. Engl.* **32:**1489–1491.
Schleucher, J., Schwendinger, M., Sattler, M., Schmidt, P., Schedletzky, O., Glaser, S. J., Sorensen, O. W., and Griesinger, C., 1994, *J. Biomol. NMR* **4:**301–306.
Schramm, S., and Oldfield, E., 1983, *Biochemistry* **22:**2908–2913.
Seeholzer, S. H., Cohn, M., Putkey, J. A., Means, A. R., and Crespi, H. L., 1986, *Proc. Natl. Acad. Sci. USA* **83:**3634–3638.
Seelig, J., 1977, *Quart. Rev. Biophys.* **10:**363–418.
Shan, X., Gardner, K. H., Muhandiram, D. R., Rao, N. S., Arrowsmith, C. H., and Kay, L. E., 1996, *J. Am. Chem. Soc.* **118:**6570–6579.
Shirakawa, M., Wälchli, M., Shimizu, M. and Kyogoku, Y., 1995, *J. Biomol. NMR* **5:**323–326.
Sippl, M., 1995, *Curr. Opin. Struct. Biol.* **5**:229–235.
Skolnick, J., Kolinski, A., and Ortiz, A. R., 1997, *J. Mol. Biol.* **265:**217–241.
Smith, B. O., Ito, Y., Raine, A., Teichmann, S., Ben-Tovim, L., Nietlispach, D., Broadhurst, R. W., Terada, T., Kelly, M., Oschkinat, H., Shibata, T., Yokoyama, S., and Laue, E. D., 1996, *J. Biomol. NMR* **8:**360–368.
Spera, S., and Bax, A., 1991, *J. Am. Chem. Soc.* **113:**5490–5492.
Stonehouse, J., Shaw, G. L., Keeler, J., and Laue, E. D., 1994, *J. Magn. Reson. A* **107:**178–184.
Tjandra, N., and Bax, A., 1997, *J. Magn. Reson.* **124:**512–515.
Tjandra, N., Grzesiek, S., and Bax, A., 1996, *J. Am. Chem. Soc.* **118:**6264–6272.
Tjandra, N., Garrett, D. S., Gronenborn, A. M., Bax, A., and Clore, G. M., 1997a, *Nature Struct. Biol.* **4:**443–449.
Tjandra, N., Omichinski, J. G., Gronenborn, A. M., Clore, G. M., and Bax, A., 1997b, *Nature Struct. Biol.* **4:**732.
Tolbert, T. J., and Williamson, J. R., 1996, *J. Am. Chem. Soc.* **118:**7929–7940.
Tolman, J. R., Chung, J., and Prestegard, J. H., 1992, *J. Magn. Reson.* **98:**462–467.
Tolman, J. R., Flanagan, J. M., Kennedy, M. A., and Prestegard, J. H., 1995, *Proc. Natl. Acad. Sci. USA* **92:**9279–9283.
Torchia, D. A., Sparks, S. W., and Bax, A., 1988a, *J. Am. Chem. Soc.* **110:**2320–2321.
Torchia, D. A., Sparks, S. W., and Bax, A., 1988b, *Biochemistry* **27:**5135–5141.
Tsang, P., Wright, P. E., and Rance, M., 1990, *J. Am. Chem. Soc.* **112:**8183–8185.
Venters, R. A., Huang, C.-C., Farmer, B. T., II, Trolard, R., Spicer, L. D., and Fierke, C. A., 1995a, *J. Biomol. NMR* **5:**339–344.
Venters, R. A., Metzler, W. J., Spicer, L. D., Mueller, L., and Farmer, B. T., II, 1995b, *J. Am. Chem. Soc.* **117:**9592–9593.
Venters, R. A., Farmer , B. T., II, Fierke, C. A., and Spicer, L. D., 1996, *J. Mol. Biol.* **264:**1101–1116.
Vold, R. R., and Vold, R. L., 1991, *Adv. Magn. Opt. Reson.* **16:**85–171.

Vuister, G. W., and Bax, A., 1992, *J. Magn. Reson.* **98:**428–435.
Vuister, G. W., Clore, G. M., Gronenborn, A. M., Powers, R., Garrett, D. S., Tschudin, R., and Bax, A., 1993, *J. Magn. Reson. B* **101:**210–213.
Waugh, D. S., 1996, *J. Biomol. NMR* **8:**184–192.
Werbelow, L. G., and Grant, D. M., 1977, *Adv. Magn. Reson.* **9:**189–299.
Wishart, D. S., and Sykes, B. D., 1994, *J. Biomol. NMR* **4:**171–180.
Wishart, D. S., Sykes, B. D., and Richards, F. M., 1991, *J. Mol. Biol.* **222:**311–333.
Wüthrich, K., 1986, *NMR of Proteins and Nucleic Acids*, Wiley, New York.
Yamazaki, T., Lee, W., Arrowsmith, C. H., Muhandiram, D. R., and Kay, L. E., 1994a, *J. Am. Chem. Soc.* **116:**11655–11666.
Yamazaki, T., Lee, W., Revington, M., Mattiello, D. L., Dahlquist, F. W., Arrowsmith, C. H., and Kay, L. E., 1994b, *J. Am. Chem. Soc.* **116:**6464–6465.
Yamazaki, T., Muhandiram, D. R., and Kay, L. E., 1994c, *J. Am. Chem. Soc.* **116:**8266–8278.
Yamazaki, T., Tochio, H., Furui, J., Aimoto, S., and Kyogoku, Y., 1997, *J. Am. Chem. Soc.* **119:**872–880.
Yang, D., and Kay, L. E., 1996, *J. Magn. Reson. B* **110:**213–218.
Yang, D., Mittermaier, T., Mok, Y. K., and Kay, L. E., 1998, *J. Mol. Biol.* **276:**939–954.
Yu, L., Petros, A. M., Schnuchel, A., Zhong, P., Severin, J. M., Walter, K., Holzman, T. F., and Fesik, S. W., 1997, *Nature Struct. Biol.* **4:**483–489.
Zhang, H., Zhao, D., Revington, M., Lee, W., Jia, X., Arrowsmith, C., and Jardetzky, O., 1994, *J. Mol. Biol.* **238:**592–614.
Zhao, D., and Jardetzky, O., 1994, *J. Mol. Biol.* **239:**601–607.

3

NMR of Perdeuterated Large Proteins

Bennett T. Farmer II and Ronald A. Venters

1. INTRODUCTION AND HISTORICAL PERSPECTIVE

1.1. Assignment and Structural Studies of Larger Proteins

1.1.1. ^{1}H Only

Ever since the first sequential ^{1}H NMR assignment of a protein was reported (Wagner and Wüthrich, 1982), considerable effort has been expended to increase the size of proteins that can be studied by high-resolution NMR spectroscopy. To date, ^{1}H homonuclear 2D NMR has provided both chemical-shift assignments and three-dimensional solution-state structures at atomic resolution for numerous peptides and small proteins (Barlow *et al.*, 1993; Davis *et al.*, 1993; Senn and Klaus, 1993; Kallen *et al.*, 1991). However, ^{1}H homonuclear 2D methodologies are fundamentally constrained to a maximum protein size of ~10 kDa. Although protein size, in kilodaltons, is typically used to categorize the ability of NMR to provide three-dimensional structures, for ^{1}H homonuclear 2D NMR, a more relevant parameter is the total number of protons in the protein.

Bennett T. Farmer II • Macromolecular NMR, Pharmaceutical Research Institute, Bristol-Myers Squibb, Princeton, New Jersey 08543-4000. **Ronald A. Venters** • Duke University Medical Center, Durham, North Carolina 27710.

Biological Magnetic Resonance, Volume 16: Modern Techniques in Protein NMR, edited by Krishna and Berliner. Kluwer Academic / Plenum Publishers, 1999.